AD_____

Award Number: DAMD17-98-1-8281

TITLE: Molecular Basis of the Response to Radiation

PRINCIPAL INVESTIGATOR: Sharon E. Plon, M.D., Ph.D.

CONTRACTING ORGANIZATION: Baylor College of Medicine
Houston, Texas 77030

REPORT DATE: June 2002

TYPE OF REPORT: Final Addendum

PREPARED FOR: U.S. Army Medical Research and Materiel Command
Fort Detrick, Maryland 21702-5012

DISTRIBUTION STATEMENT: Approved for Public Release;
Distribution Unlimited

REPORT DOCUMENTATION PAGE

Form Approved
OMB No. 074-0188

1. AGENCY USE ONLY (Leave blank)	2. REPORT DATE	3. REPORT TYPE AND DATES COVERED
	June 2002	Final Addendum (26 May 01 - 25 May 02)

4. TITLE AND SUBTITLE
Molecular Basis of the Response to Radiation

5. FUNDING NUMBERS
DAMD17-98-1-8281

6. AUTHOR(S)
Sharon E. Plon, M.D., Ph.D.

7. PERFORMING ORGANIZATION NAME(S) AND ADDRESS(ES)
Baylor College of Medicine
Houston, Texas 77030

E-Mail: splon@bcm.tmc.edu

8. PERFORMING ORGANIZATION REPORT NUMBER

9. SPONSORING / MONITORING AGENCY NAME(S) AND ADDRESS(ES)
U.S. Army Medical Research and Materiel Command
Fort Detrick, Maryland 21702-5012

10. SPONSORING / MONITORING AGENCY REPORT NUMBER

11. SUPPLEMENTARY NOTES

12a. DISTRIBUTION / AVAILABILITY STATEMENT
Approved for Public Release; Distribution Unlimited

12b. DISTRIBUTION CODE

13. ABSTRACT ***(Maximum 200 Words)***

This three year IDEA Award with a one year no cost extension has been completed. We have made progress towards all three Technical Objectives. We encountered scientific problems isolating novel cDNAs encoding human homologs of yeast DNA damage response genes *RAD9* and *DUN1* during year 1 and year 2. In contrast, two hybrid screens resulted in the isolation of human homologs of *RAD18* and *RAD21* and the focus over years 2, 3 and 4 has been the characterization of the human Rad21 protein in mammalian cells and it's degradation in response to DNA damage.

Alterations in expression of human Rad21 mRNA and protein in human breast cancer cell lines were detected. We also demonstrated that Rad21 is cleaved upon induction of the apoptotic pathway (as opposed to DNA damage itself). The cleavage site has been biochemically identified, characteristics of the cleavage enzyme determined and cellular localization of the cleaved proteins performed. The carboxy terminal Rad21 cleavage product has a pro-apoptotic effect on murine mammay cells generating a positive feedback loop in apoptosis. A manuscript describing this regulation of the mammalian Rad21 protein has been submitted and is currently under review.

14. SUBJECT TERMS	15. NUMBER OF PAGES
breast cancer	59
	16. PRICE CODE

17. SECURITY CLASSIFICATION OF REPORT	18. SECURITY CLASSIFICATION OF THIS PAGE	19. SECURITY CLASSIFICATION OF ABSTRACT	20. LIMITATION OF ABSTRACT
Unclassified	Unclassified	Unclassified	Unlimited

Table of Contents

A. Introduction

The goal of this project is to further define at a molecular level the human gene products required for the normal cell cycle response after DNA damage. The checkpoint response is a fundamental mechanism by which cells control their cell division cycle after experiencing DNA damage from radiation. This response results in an arrest in the G1, S and G2 phases of the cycle until damage is repaired. This checkpoint response is conserved among eukaryotes including the budding yeast *Saccharomyces cerevisiae*. Human cells have an additional response which results in apoptosis after DNA damage. In our application, we proposed to exploit the conservation between yeasts and humans to isolate human checkpoint genes by large scale complementation screens and homology searches isolating novel human cDNAs which can complement yeast G2 checkpoint mutant strains. Subsequent Technical Objectives were directed towards understanding the structure and expression of these genes in both normal and malignant mammary cells. The final Technical Objective was to assay changes in expression of these genes after DNA damage. In this final report we detail progress during the four years (including a no-cost extension during the fourth year) of this award towards all three objectives. This grant was co-funded with a companion CDA Award for the PI, Dr. Sharon Plon (grant #DAMD17-97-1-7284).

B. Progress toward completing the proposed Technical Objectives.

RESULTS

Technical Objective 1 - Isolation of additional human G2 checkpoint genes.

a. **Complementation Assay:** As previously described, this work comprised the first year of the IDEA award. Human cDNA libraries were screened by expression in yeast *rad9, cdc9-8* and *mec1, cdc9-8* strains as described in the application. Despite extensive screening no human cDNAs which could reproducibly rescue the checkpoint defect of these strains was identified

b. **Sequence Identity:** As described in the year 1 progress report, a second approach to isolating human checkpoint genes utilized homologous regions between evolutionarily distant species (*S. cerevisiae and S. pombe)* to develop degenerate PCR based primers. For example, a fission yeast homolog of *RAD9* named *rhp9* was published. Alignment of those sequences revealed areas of homology that may suggest conserved regions of the protein. One such area is in the carboxy terminus consistent with the known BRCT domain. During year 1 we made a major effort to develop a series of degenerate PCR primers to these regions but the amplified sequences obtained did not demonstrate additional regions of homology to the *S. cerevisiase RAD9* or *DUN1* genes. We proposed to try direct amplification from human mammary cDNA and mammary carcinoma cDNA in order to prevent any bias against long messages or "unclonable" sequences that might not be represented in a cDNA library.

During year 2, amplification was performed on multiple human cDNA samples including normal mammary cells, breast carcinoma cell lines and ovarian cDNA. The resulting PCR products were cloned and sequenced. No sequences obtained provided evidence for additional regions of homology between the isolated sequence and the yeast *RAD9* or *DUN1* genes respectively. Thus, the use of direct cDNA sources from either benign or malignant mammary cells did not result in isolation of novel human cDNAs for these checkpoint genes. During year three of the grant the human genome project neared completion and searches of these resources using a variety of techniques has not identified human genes or cDNAs with significant homology (outside the BRCT domain) for *RAD9* and *DUN1*. Thus, these two genes may not have a direct homolog in the human genome, but their functions appear to be carried out by other proteins which do not show extensive sequence homology, e.g., p53 in the case of Dun1 and BRCA1 for Rad9.

c. Isolation of human *RAD21* cDNA.

We used a different form of genetic screen including two-hybrid screens in yeast for human cDNAs in the DNA damage checkpoint and repair response have been accomplished. As part of those screens cDNAs encoding the human homolog of *S. pombe RAD21* and *S. cerevisiae RAD18* were isolated. The *RAD21* sequence had been previously reported in the literature although the human gene and protein had not been thoroughly characterized. Much of the remainder of this project then focused on studies of the human *RAD21* gene and the regulation of the Rad21 protein encoded by that gene in response to DNA damage.

Technical Objective 2A – Checkpoint gene structure and expression in human breast cancer cell lines.

As accomplished during year 1 of this grant, RNA, DNA and protein were derived from eight human mammary derived cell lines, MCF10A, MCF7, MDA-MB-157, MDA-MD-231, MDA-MB-136, BT-20, HBL100 and SKBR-3 grown in culture under controlled conditions. Analysis of expression of *RAD21* reveals increased expression at the RNA level in some breast cancer cell lines, specifically MDA-MB-436 and SK-BR-3 in comparison to the HMEC controls.

We then pursued the development of reagents in order to study the expression of human Rad21 in mammary cell lines and breast cancer samples. A polyclonal antibody was obtained towards the end of year 1. During year 2, we obtained a large stock of this anti-sera and obtained affinity purified antibody that is being used in immunohistochemistry and immunoflourescence experiments. We also isolated a monoclonal antisera for additional studies (eg, immunoprecipitation with polyclonal antisera followed by Western blotting with monoclonal antibody). Monoclonal antibody which recognizes the human Rad21 protein was obtained by immunization with a GST-Rad21 fusion protein. The monoclonal is functional in both Western blot and immunoprecipitation assays.

During year 2, we also performed Western blots analysis of the cell lines listed above with the anti-Rad21 polyclonal antibody. Expression of Rad21 is variable in human breast cancer cell lines. In particular, the level of Rad21 protein is elevated in MCF-7 and SK-BR-3 cell lines in comparison to MCF10F cells. In contrast Rad21 protein is absent in the BT-20 cell line suggesting a possible mutational mechanism. These results provided a rationale for further analysis of Rad21 protein expression in human breast cancers with known levels of aneuploidy.

In order to accomplish this last goal, during year 3, we collaborated with the Baylor Breast Cancer Center (Kent Osborne, Director). They tested the anti-Rad21 antibody on a pilot sample of breast cancer samples and optimized the protocol to provide excellent detection by immunohistochemistry after antigen retrieval. We planned during year 4 to systematically determine the expression of Rad21 in breast cancer samples as a function of chromosome number or aneuploidy. However, because of delays in studies of breast cancer tissues secondary to Tropical Storm Allison these studies are continuing after completion of this grant..

Technical Objective 3 - Determination of Changes in Response to Radiation of a Human Breast Cancer Cell Line upon Expression of Human Checkpoint Genes.

We used cDNA probes and antisera to study Rad21 expression in normal and checkpoint deficient cell lines after DNA damage as originally described in the grant application. *RAD21* mRNA is not up or down regulated in response to ionizing radiation. Western analysis revealed that after ionizing radiation there was no change in the major bands representing Rad21 in several cell types including the totally checkpoint deficient A-T cells. Thus, we did not see evidence for a change in phosphorylation or expression after ionizing radiation. However, some cell types demonstrated the production of a lower molecular weight band consistent with cleavage.

Further analysis revealed that cells in the early stages of apoptosis demonstrated cleavage of the endogenous Rad21 protein. Detailed description of the experiments summarized in this section can be found in Appendix 4 which is a manuscript currently under review for the journal *Molecular and Cellular Biology*, entitled "Linking Sister Chromatid Cohesion and Apoptosis: Role of Rad21".

Induction of apoptosis in multiple human cell lines including the MCF7 breast cancer cell line and EL-4 mammary epithelial cells results in the early (4 hours post insult) generation of a 64 kD cleavage Rad21 product. Identity of this product is confirmed by recognition by affinity purified polyclonal and monoclonal antibody to human Rad21. This product is detected after induction of apoptosis by both DNA damaging agents (ionizing radiation and topoisomerase inhibitors) as well as non-DNA damaging agents (cycloheximide treatment and cytokine withdrawal). Induction of apoptosis is assayed by cleavage of the endogenous PARP protein and morphological changes consistent with apoptosis. In addition, equivalent doses of ionizing radiation in cells that are resistant to apoptosis do not generate this band; thus, it is not a simple byproduct of DNA damage. Addition of caspase inhibitors to the cells blocks the cleavage of Rad21 after an apoptotic signal.

The finding that Rad21 is regulated during apoptosis (as opposed to DNA damage itself) is a novel finding. This has lead to a new hypothesis that there may be a direct link between the development of aneuploidy (given Rad21's role in chromosome cohesion) and apoptosis. During year 3 we used our biochemical reagents to purify the cleaved fragment. The isolated peptides were then sequenced in order to determine the specific cleavage site within the protein. This site is unique from the previously identified cleavage of Rad21 that oocurs at the end of mitosis. We have also identified that the cleavage is sensitive to the presence of a particular set of phosphatase inhibitors. Future biochemical experiments will focus on identifying the specific caspase-like activity which is responsible for Rad21 cleavage.

Given the role of rad21 in chromosome cohesion, we hypothesized that the cleavage product may signal subsequent events of apoptosis including DNA degradation. Further evidence for this is provided by the finding that the Rad21 cleavage product derived from the carboxy terminus is translocated to the cytoplasm after cleavage. Most recently, during year 4 we have demonstrated that forced expression of the carboxy terminal fragment in mammary cells causes pro-apoptotic activity including an increase in endogenous caspase activity. Thus, there is a positive feedback loop resulting from early induction of Rad21 cleavage after apoptotic stimuli.

Personnel Supported by this Award over the Term of the Grant

Debananda Pati - Assistant Professor
Anu Gannavarapu - Research Assistant II
Allison Franz - Research Technician II
Amy Barbour - Lab Assistant
Luke Engelking - Lab Assistant
Margot Perez - Research Associate
Shirong Luo - Research Tech III
Rita Wilkerson - Lab Tech II

C. Key Research Accomplishments

- Extensive degenerate PCR cloning to obtain human homologs of *RAD9* and *DUN1* completed utilizing cDNA sources from both normal mammary cells and breast carcinoma cells.
- Polyclonal antibody to human Rad21 protein produced and affinity purified.
- Monoclonal antibody to human Rad21 protein produced.
- Determined expression of Rad21 protein assayed in human mammary and breast cancer cell lines.
- Development and optimization of technique to assay Rad21 expression in human breast cancers accomplished.
- Identification of Rad21 cleavage as an early step in apoptosis.
- Identification of Rad21 cleavage site after induction of apoptosis.
- Determination that carboxy terminal fragment of Rad21 has a pro-apoptotic effect on mammary cells.

D. Reportable Outcomes:

- Results of this project presented at four meetings:
- International Meeting on Forkhead/Winged Helix Proteins" Analysis of *CHES1*, A Human Checkpoint Suppressor," Scripps Institute, La Jolla, CA, November, 1998
- Cold Spring Harbor Cell Cycle Meeting, May, 2000, Cold Spring Harbor, New York (abstract attached).
- DOD Era of Hope Meeting, June 2000, Atlanta GA.
- Cold Spring Harbor Cell Cycle Meeting, May, 2002, Cold Spring Harbor, New York (abstract attached).
- Monoclonal antibody to human Rad21 protein produced.
- Manuscript entitled "Linking Sister Chromatid Cohesion and Apoptosis: Role of Rad21" submitted to *Molecular and Cellular Biology.*
- DOD Breast Cancer Research Program Concept, IDEA award and CDA award grant applications were selected for award to co-Investigator, Debananda Pati, to explore the newly identified link between apoptosis and chromosome cohesion.

E. Conclusions

The most challenging aspect of this project was the isolation of novel cDNAs encoding human homologs of yeast DNA damage response genes. Complementation of the yeast mutant *rad9* did not yield human cDNAs with significant homology. Major efforts to isolate cDNAs by degenerate PCR strategies for *RAD9* and *DUN1* during year 1 and year 2 were also not successful and analysis of the human genome sequence suggests that these homologs may not exist. In contrast, two hybrid screens using known human DNA damage response/cell cycle genes did result in the isolation of human homologs of *RAD18* and *RAD21.* Thus, the focus over year 2 and 3 has been the characterization of the human Rad21 protein in mammalian cells and breast cancer cells.

The subsequent objectives focused on determination of whether cDNAs isolated in genetic screens are altered in expression or structure in breast cancers. As described above we do see alterations in expression of human Rad21 mRNA and protein in human breast cancer cell lines. This has lead to development of immunohistochemistry techniques and ongoing experiments on primary human breast cancer samples with the Baylor Breast Care Center investigators. These studies will in particular look for a correlation between Rad21 expression and aneuploidy.

The results of Technical Objective 3 have been most surprising to date. We did not see alteration in *RAD21* mRNA or Rad21 phosphorylation in human cells exposed to DNA damage. However, we did detect specific cleavage of the protein. This has lead to determination that induction of the apoptotic pathway (as opposed to DNA damage itself) induces specific cleavage of the human Rad21 cohesin protein. The biochemical characteristics of the cleavage have been identified and the cleavage site in the protein determined. This cleavage product stimulates subsequent events in apoptosis and may result in aneuploidy in cells that survive the apoptotic response. Thus, these results suggest that when a cell makes a decision to undergo apoptosis (either due to endogenous damage or response to chemotherapy) it acts to destroy proteins required for DNA repair, including Rad21. The byproducts of this destruction further stimulate apoptosis. However, cells which survive this process are highly likely to demonstrate genomic instability (and thus be potentially more tumorigenic) due to the loss of the pathways which are designed to maintain a normal chromosome content.

Appendix 1 – Abstract from Cold Spring Harbor Laboratories – Cell Cycle Meeting, 2000

CLEAVAGE OF HUMAN Rad21 COHESIN PROTEIN: POTENTIAL ROLE IN EARLY APOPTOSIS

DEBANANDA PATI, Sharon E. Plon
Department of Pediatrics, Baylor College of Medicine, Houston, TX

Sister chromatid cohesion during DNA replication plays a pivotal role for accurate chromosome segregation in eukaryotic cell cycle. Analysis of Rad21 function in fission yeast and *SCC1/MCD1* in budding yeast have demonstrated that it is required for appropriate chromosome segregation during normal mitotic cell cycles and double strand break repair after DNA damage. In budding yeast sister chromatid separation is promoted by the cleavage of the cohesin sub-unit Scc1 and may involve ubiquitin-mediated proteolysis of regulatory molecules. In a two-hybrid screen for potential targets of human Cdc34 (hCdc34) ubiquitin-conjugating enzyme, we have isolated human Rad21 (hRad21) as an hCdc34 interactor. Transfection studies in mammalian cells have indicated physical association of hCdc34 and hRad21 using co-immunoprecipitation experiments. Level of hRad21 was significantly enhanced in the presence of proteasome inhibitors, indicating the involvement of ubiquitin-mediated proteolysis. In a parallel set of studies to analyze the role of Rad21 in mammalian cells after DNA damage, we have identified a novel regulation of hRad21 protein in apoptosis. Induction of apoptosis in multiple human cell lines results in the early (4 hours post insult) generation of a 64kDa cleavage hRad21 product. Although Rad21 is a nuclear protein the cleaved 64 kDa product is found in both nuclear and cytoplasmic fractions. Identity of this product is confirmed by recognition by affinity purified polyclonal and monoclonal antibody to hRad21. This product is detected after induction of apoptosis by both DNA damaging agents (ionizing radiation and topoisomerase inhibitors) as well as non-DNA damaging agents (cycloheximide treatment and cytokine withdrawal). In addition, equivalent doses of ionizing radiation in cells which are resistant to apoptosis do not generate this band; thus, it is not a simple byproduct of DNA damage. Given the role of Rad21 in chromosome cohesion, this cleavage product may signal subsequent events of apoptosis including DNA degradation. A role for Rad21 in apoptosis has been further strengthened by identification of a number of genes involved in apoptosis as interactors of hRad21 in a two-hybrid assay. In summary, ubiquitin-mediated proteolysis may play a role in the cleavage of hRad21 during metaphase-anaphase transition. In addition to previously described functions of Rad21 in chromosome segregation and DNA repair, cleavage of the protein is an early event in the apoptotic pathway. These results provide the framework to identify the physiologic role of hRad21 function in the apoptotic response of normal and malignant cells.

Appendix 2 – Abstract from DOD Era of Hope Meeting – 2000.

CHARACTERIZATION OF THE HUMAN RAD21 COHESIN PROTEIN AND DETECTION OF SPECIFIC CLEAVAGE EARLY IN APOPTOSIS

Drs. Sharon E. Plon and Debananda Pati

Department of Pediatrics, Baylor College of Medicine, Houston, TX 77030

E-mail: splon@txccc.org

The goal of this project is to identify human homologs of yeast genes proven to play a role in the response to DNA damage. Isolation of these genes will then allow characterization of their expression and activity in both normal and malignant cells exposed to DNA damage. Our laboratory has employed a number of techniques to identify human homologs of these genes including yeast two hybrid screens with human cell cycle genes. We have identified the human homolog of the yeasts Rad21/*SCC1/MCD1* genes. Prior analysis of Rad21 function in fission yeast and *SCC1/MCD1* in budding yeast have demonstrated that it is required for double strand break repair after DNA damage and appropriate chromosome segregation during normal mitotic cell cycles.

We have now characterized the expression of human Rad21 RNA and protein in mammalian cells in response to DNA damage and in human breast cancer cell lines. Expression of Rad21 is variable in human breast cancer cell lines. In particular, the level of Rad21 protein is elevated in MCF-7 and SK-BR-3 cell lines in comparison to MCF10F cells. In contrast Rad21 protein is absent in the BT-20 cell line suggesting a possible mutational mechanism. These results provide a rationale for further analysis of Rad21 protein expression in human breast cancers with known levels of aneuploidy. Analysis of mammalian cells after DNA damage has identified a novel regulation of Rad21 protein in apoptosis. Induction of apoptosis in multiple human cell lines results in the early (4 hours post insult) generation of a 64 kD cleavage Rad21 product. Identity of this product is confirmed by recognition by affinity purified polyclonal and monoclonal antibody to human Rad21. This product is detected after induction of apoptosis by both DNA damaging agents (ionizing radiation and topoisomerase inhibitors) as well as non-DNA damaging agents (cycloheximide treatment and cytokine withdrawal). In addition, equivalent doses of ionizing radiation in cells which are resistant to apoptosis do not generate this band; thus, it is not a simple byproduct of DNA damage. Given the role of rad21 in chromosome cohesion, this cleavage product may signal subsequent events of apoptosis including DNA degradation. In summary, expression of the human cohesin protein Rad21 is altered in human breast cancer cell lines and in addition to previously described functions in chromosome segration and DNA repair, cleavage of the protein is an early event in the apoptotic pathway. These results provide the framework to identify the importance of Rad21 function in the apoptotic response of breast cancer cells to treatment.

The U.S. Army Medical Research and Materiel Command under DAMD17-97-1-7284 and DAMD17-98-8281 supported this work.

Appendix 3 – Abstract from Cold Spring Harbor Laboratories – Cell Cycle Meeting, 2002

LINKING SISTER CHROMATID COHESION TO APOPTOSIS: ROLE OF hRAD21

DEBANANDA PATI and Sharon E. Plon
Department of Pediatrics, Baylor College of Medicine, Houston, TX

Sister chromatid cohesion during DNA replication plays a pivotal role in accurate chromosome segregation in the eukaryotic cell cycle. Rad21 is one of the major cohesin subunits keeping sister chromatids together until anaphase, when proteolytic cleavage by separase allows the chromosomes to separate. Mitotic cleavage sites in Rad21 in yeast as well as humans have been mapped. Here we have shown that human Rad21 (hRad21) is also cleaved during apoptosis, induced by various agents including DNA damaging (ionizing radiation and topoisomerase inhibitors) as well as non-DNA damaging agents (cycloheximide treatment and cytokine withdrawal). Recognition by affinity-purified polyclonal and monoclonal antibody to hRad21 confirms the identity of the cleavage product. We have mapped the apoptotic cleavage site in hRad21, which is distinct from the mitotic cleavage sites previously described. The apoptotic cleavage site is conserved among vertebrate species, and cleavage is likely to be mediated by Caspase 3. Cleavage of hRad21 appears to be an early event in the apoptosis pathway. Induction of apoptosis in multiple human cell lines results in the early (4 hours post insult) generation of 64kDa and 60kDa hRad21 cleavage products. Although hRad21 is a nuclear protein, the cleaved 64kDa product is found in both nuclear and cytoplasmic fractions. While hRad21 is cleaved by various apoptotic agents, equivalent doses of ionizing radiation in cells which are resistant to apoptosis do not generate cleavage band; thus, is not a simple byproduct of DNA damage. Given the role of hRad21 in chromosome cohesion, this cleavage product may signal subsequent events of apoptosis including DNA degradation. A role for hRad21 in apoptosis has been further strengthened by identification of a number of genes involved in apoptosis as interactors of hRad21 in a two-hybrid assay not described in the present study. In summary, in addition to previously described functions of hRad21 in chromosome segregation and DNA repair, cleavage of the protein is an early event in the apoptotic pathway. These results provide the framework to identify the physiologic role of hRad21 in the apoptotic response of normal and malignant cells.

Appendix 4 - Manuscript submitted for publication to *Molecular and Cellular Biology*

Pati et al. Linking Sister Chromatid Cohesion and Apoptosis: Role of Rad21

Linking Sister Chromatid Cohesion and Apoptosis: Role of Rad21

Debananda Pati*, Nenggang Zhang, and Sharon E. Plon

Texas Children's Cancer Center, Department of Pediatrics, Baylor College of Medicine,

Houston, TX 77030, USA

Running title: Cohesin Rad21 and apoptosis

All correspondence should be addressed to:

Debananda Pati, Ph.D.

Texas Children's Cancer Center

Baylor College of Medicine

6621 Fannin St., MC 3-3320

Houston, TX 77030, USA

Tel: 832-824-4575; Fax: 832-825-4202

E-Mail: pati@bcm.tmc.edu

Word count for the Materials and Methods Section: 1,854

Word count for the Introduction, Results and Discussion section: 3,395

ABSTRACT

Rad21 is one of the major cohesin subunits that holds sister chromatids together until anaphase, when proteolytic cleavage by separase, a caspase-like enzyme, allows chromosomal separation. We show that cleavage of human Rad21 (hRad21) also occurs during apoptosis induced by diverse stimuli. Induction of apoptosis in multiple human cell lines results in the early (4 hours post insult) generation of 64 kDa and 60 kDa carboxy terminal hRad21 cleavage products. We biochemically mapped a apoptotic cleavage site at residue Asp (D)^{279} of hRad21. This apoptotic cleavage site is distinct from mitotic cleavage sites previously described. Although hRad21 is cleaved *in vitro* at D^{279} by caspase-3 and –7, indirect evidence suggests involvement of a novel caspase or caspase-like molecule in hRad21 cleavage. hRad21 is a nuclear protein, however, the cleaved 64 kDa carboxy-terminal product is translocated to the cytoplasm early in apoptosis before chromatin condensation and nuclear fragmentation. Overexpression of the 64 kDa cleavage product results in apoptosis in Molt4 and MCF-7 cells. Given the role of hRad21 in chromosome cohesion, the cleaved C-terminal product and its translocation to the cytoplasm may act as a nuclear signal for apoptosis. In summary, we show that cleavage of a cohesion protein and translocation of the C-terminal cleavage product to the cytoplasm are early events in the apoptotic pathway and cause amplification of the cell death signal in a positive feed back manner by activation of more caspases.

INTRODUCTION

Normal development and homeostasis require the orderly regulation of both cell proliferation and cell survival. Cell cycle progression and control of apoptosis are thought to be intimately linked processes. Activation of the cell cycle plays a significant role in the regulation of apoptosis (16); in some cell types and under certain conditions, apoptosis has been shown to occur only at specific stages of the cell cycle (24). Mitosis and apoptosis are also closely interrelated (25), and the mitotic index is the most important determinant of the apoptotic index (25). Although proteins that regulate apoptosis have been implicated in restraining cell cycle entry (14) and controlling ploidy (29), the effector molecules at the interface between cell proliferation and cell survival have remained elusive.

Studies in yeast and higher eukaryotes including humans have indicated that an evolutionarily conserved protein complex, called cohesin, and its subunit Mcd1/Scc1/hRad21 are required for appropriate arrangement of chromosomes during normal cell division (11, 28, for review see 20, 30, 31, 36). Analyses of Rad21 function in fission yeast, *S. pombe*, and Scc1/Mcd1 function in budding yeast, *S. cerevisiae*, demonstrate that the nuclear phosphoprotein is required for appropriate chromosomal cohesion during the mitotic cell cycle and double strand break repair after DNA damage (2, 30). Biochemical analysis of cohesin indicates that it acts as a molecular glue, and human cohesin can promote intermolecular DNA catenation, a mechanism that links two sister chromatids togather (26). In budding yeast, loss of cohesion at the metaphase-anaphase transition is accompanied by proteolytic cleavage of the Scc1/Mcd1 protein (11, 28, 30, 37) followed by its dissociation from the chromatids (28, 30). Cleavage depends on a CD clan endopeptidase, Esp1 (also known as separin/separase) (37, 38), which is complexed

with its inhibitor Pds1 (securin) before anaphase (23, 39). In metaphase, ubiquitin-mediated degradation of the securin protein by APC/C-Cdc20 ubiquitin-ligase releases separin protein, which proteolytically cleaves cohesin Rad21, thereby releasing the sister chromatids (7, 8, 10, 18, 42). In budding yeast, fission yeast, and human cells, Rad21 has two mitotic cleavage sites for separase (12, 37, 38), and cleavage by separase appears to be essential for sister chromatid separation and for the completion of cytokinesis (12). In contrast to the simultaneous release of cohesin from the chromosome arms and centomere region in budding yeast by separase cleavage, in metazoans, most cohesin is removed in early prophase from chromosome arms by a cleavage-independent mechanism (12, 39, 40). Only residual amounts of cohesin are cleaved at the onset of anaphase, coinciding with its disappearance from centromeres. Thus, Scc1/Mcd1/Rad21 plays a critical role in the eukaryotic cell division cycle by regulating sister chromatid cohesion and separation at the metaphase to anaphase transition.

Our results indicate that in addition to establishing and maintaining sister chromatid cohesion during mitosis, hRad21 plays a role in apoptosis, and its cleavage during apoptosis may act as a nuclear signal to initiate cytoplasmic events involved in the apoptotic pathway.

MATERIALS AND METHODS

Plasmids: Full length *hRAD21* cDNA plasmid (KIAA 0078) in pBluescript SK+ vector was obtained from Kazusa DNA Research Institute, Chiba, Japan. Full length *hRAD21* cDNA was subcloned into several mammalian expression plasmids including pFLAGCMV2, pCS2MT and pCDNA6Myc-HisC to produce epitope-tagged proteins where applicable. The following plasmids were used for transfection: pCS2MT-*hRAD21* was constructed by ligation of the 2331 bp NcoI/DraI fragment bearing the *hRAD21* cDNA, in frame to the end of the 6th myc epitope in pCS2MT (B. Kelley, Fred Hutchinson Cancer Center, Seattle, WA). pFLAGCMV2-*hRAD21* was generated by cloning the full length *hRAD21* gene contained on a 2578 bp MScI/StuI fragment from pSKKIAA0078 into pFLAGCMV2 (Kodak) that was digested with SmaI.

Site-directed mutagenesis of hRad21: pcS2MT-*hRAD21* apoptotic cleavage site (ACS) mutant-I (PDSPD^{279}S to PDSPA^{279}S) and mutant-II (PD^{276}S^{277}PD^{279}S^{280} to PA^{276}A^{277}PA^{279}A^{280}) were generated using a PCR based site-directed mutagenesis protocol as previously described (33). The PCR reaction resulted in a 550 bp internal *hRAD21* fragment containing the mutations. A 221 bp piece of wild type (WT) *hRAD21* (from BsgI to PFLFI sites) was replaced with the comparable mutated fragment. The resulting plasmids, pCS2MT-*hRAD21*-ACS mut-I and pCS2MT-*hRAD21*-ACS mut-II were verified by DNA sequencing. The amino terminal (N-hRad21, encoding amino acids 1-279) and carboxy terminal (C-hRad21, encoding amino acids 280-631) cleavage products were cloned into myc epitope-tagged pCS2MT vectors using PCR amplification of the fragments from the *hRAD21* cDNA. These constructs were also verified by DNA sequencing.

Generation of hRad21 polyclonal and monoclonal antibodies: Rabbit polyclonal antibody (pAb) were raised commercially (Covance, PA) against synthetic peptides corresponding to the 14 carboxy terminal amino acid sequences of hRad21 (SDIIATPGPRFHII). Immunization and affinity purification of antibodies were performed per manufacturer's protocol. Monoclonal antibody (mAb) against a partial recombinant hRad21 protein (240 AA- 631AA) was also raised commercially from IMGENEX (San Diego, CA). Both antibodies had very high titer by ELISA testing. Both antibodies recognized the WT hRad21 protein as a specific 122 kDa band in Western blot analysis and immunoprecipitated endogenous hRad21 effectively from various human and rodent cell lines and tissue lysates. Immunodetection of the 122 kDa band was blocked competitively by pretreating the lysates with recombinant hRad21 protein or synthetic C-terminal peptides. Both antibodies were also effective in immunohistochemistry and inmmunofluorescence staining to both paraffin embedded and tissue culture slides.

Antisera: The vendors for the following monoclonal antisera were as follows: human PARP (PharMingen, San Diego, CA), Flag epitope and mouse β-actin (Sigma), c-myc epitope (9E10), bacterial trpE, caspase-3 and caspase-7 (Oncogene Research Product, Cambridge, MA). hRad21 N-terminal antibody was a gift from J-M. Peters (Research Institute of Molecular Pathology, Vienna, Austria).

Cell Cultures and Transfection: MCF-7 breast carcinoma cells, human choriocarcinoma JEG3 cells, and IMR90 primary lung fibroblast cells were obtained from American Type Culture

Collection (ATCC) and were maintained per ATCC protocol. Human Molt4 and Jurkat T-leukemia cells (both obtained from ATCC) were grown in RPMI 1640 supplemented with 10% fetal bovine serum (FBS) and maintained at 37 ^{0}C, 95% humidity and 5% CO_2. EL-12 mouse mammary epithelial cells were obtained from the Medina Laboratory (Baylor College of Medicine) and maintained as previously described (27). Cells were transfected with appropriate plasmids in 100 mm dishes using Superfect or Effectene reagents from Qiagen (Valencia, CA) per manufacturer's protocol. A fixed amount of plasmid DNA was used in any given experiment. The total amount of expression vector DNA was equalized by adding blank vectors to control for promoter competition effects. When necessary, transfection efficiency was monitored by use of 1μg pDS-Red plasmid (Clontech, Palo Alto, CA) per transfection. Transfection efficiency was determined by counting percentage of red fluorescent cells in five random fields under a microscope using appropriate fluorescent channels.

Drug Treatments: Etoposide (VP-16) (20 mg/ml injections) and camptothecin were purchased from GensiaSicor Pharmaceuticals (Irvine, CA) and Sigma (St. Louis, MO), respectively. Camptothecin was dissolved in dimethyl sulfoxide (DMSO) and stored in aliquots at –20^{0}C. Cells were plated at a concentration of 6x10^6 cells/ml and treated with appropriate concentration of drugs. Molt4 cells were treated with etoposide while Jurkat cells were treated with camptothecin for 8h unless otherwise indicated. Controls were treated with equivalent dosages of vehicle. The caspase inhibitor z-VAD-FMK was also dissolved in DMSO and stored at –20^{0}C. Peptide aldehydes MG115 and MG132 were obtained from Peptide Institute, Inc. (Lexington, KY) and dissolved at 10 mM in DMSO. Cells were treated with 0.025 mM proteasome inhibitors for 8h before harvesting. 15-deoxy-delta 12, 14-prostaglandin J_2

($15dPGJ_2$) was purchased from Cayman Chemical Co. (Ann Arbor, MI). Induction of apoptosis in JEG3 cells using $15dPGJ_2$ was carried out as described (19).

Protein Analysis and Immunoprecipitation: Cells were pelleted by low speed centrifugations (800xg for 5 min) and lysed in RIPA buffer (phosphate-buffered saline [PBS], 1% Nonidet P-40, 0.1% sodium dodecyl sulfate [SDS], 0.5% sodium deoxycholate) or PBSTDS buffer (PBS, 1% Triton X-100, 0.1% SDS, 0.5% sodium deoxycholate) containing protease and phosphatase inhibitors (1 mM EDTA, 0.2 mM phenylmethylsulfonyl fluoride, 1 μg pepstatin per ml, 30 μl aprotinin per ml, 0.5 μg leupeptin per ml, and 100 mM sodium orthovandate and 100 mM sodium fluoride) (all from SIGMA) for 10-15 min on ice, followed by passage through a 21G needle. When appropriate, additional phosphatase inhibitors cocktail I and II (Sigma) were added to the lysis buffer at a dilution of 1:100. Lysates were then centrifuged at 1000xg for 20 min, and the supernatants were aliquoted and frozen at -80^0C until use. Protein samples were also made from the cytoplasmic and nuclear fractions of apoptosis-induced Molt4 cells using protocols previously described (6). After protein quantification (using BioRad's detergent compatible protein dye and BSA as standards) and normalization, 10-40 μg of protein extracts were electrophoresed on SDS-PAGE gels and transferred to polyvinylidene difluoride (PVDF) membranes (Millipore, Bedford, MA). The filters were initially blocked with 5% nonfat-dry milk in TBST (Tris buffer saline containing 0.1% Tween 20) for 1-2h at room temperature and then probed with 1:1000 hRad21 mAb or hRad21 pAb, 1.5 μg/ml myc, 2.5 μg/ml Flag, 1:100,000 β-Actin, 1:2000 PARP antisera. The bound antibodies were visualized by the enhanced chemiluminescence (ECL) detection system (Amersham, Buckinghamshire, England), in combination with the HRP-conjugated anti-mouse or anti-rabbit secondary antibodies as

appropriate, and intensity of the specific bands in the exposed films was quantified. In some of the later studies, bound primary antibodies were detected with IRD800 dye-labeled appropriate species-specific secondary antisera and signal was visualized on a Li-Cor (Lincoln, NE) Odyssey infrared scanner. Immunoprecipitation was performed as follows: 1.0 ml of cell lysate was pre-cleared by incubation with 10 µl of normal mouse IgG and 20 µl protein G plus agarose (Oncogene Research Product, Cambridge, MA) at 4^0C for 1h on a rotator. The pre-cleared-lysate was collected after centrifugation at 800xg for 15 min. 0.5-1.0 ml of pre-cleared lysate normalized for protein concentrations was incubated at 4^0C for 1h with primary antibodies followed by addition of 20 µl Protein A/G plus agarose. The mix was then incubated at 4^0C for another 12-16h on a rotator. Precipitates were then washed four times with 1ml of ice-cold PBS with a final wash in the lysis buffer before electrophoresis and Western blot analysis.

Mapping of hRad21 apoptotic cleavage sites: Apoptosis was induced in Molt4 T-cells by treating with 10 µM etoposide for 8h. Protein lysates were subjected to immunoprecipitation using hRad21 mAb or a control bacterial trpE mAb. The immunoprecipitated samples were run on 6% SDS PAGE gels that included 0.1 mM sodium thioglycolate (Sigma) as a scavenger in the upper running buffer. Electrophoresed samples were then electroblotted onto PVDF membranes at room temperature (~25^0C) using CAPS buffer (10mM CAPS, 10% methanol, pH 11) at 400 mAmps for 45 min. At the end of the transfer, the blotted membranes were rinsed with water for 2-5 min, stained with 0.05% Coomassie blue in 1% acetic acid, 50% methanol for 5-7 min, destained in 50% methanol until the background was pale blue (5-15 min), and finally rinsed with water for 5-10 min. Appropriate bands were cut out and air-dried and sent for N-terminal sequencing by the protein chemistry core laboratory at Baylor College of Medicine.

Immunocytochemistry, DAPI staining of nuclei and detection of apoptosis: EL-12 cells were grown on FALCON culture slides. Medium was poured off before cells were treated with 0, 50, 100, 200 J/m^2 of UV. Fresh medium was added immediately after UV radiation. Cells were fixed with cold methanol after 6 h of UV treatment (unless otherwise noted). Double staining of hRad21 was performed by incubating anti-hRad21 mAb and rabbit anti C-terminal hRad21 pAb. The signals of mAb and pAb were visualized by adding rhodamine-labeled goat anti-mouse IgG (1:100) and fluorescein-labeled goat anti-rabbit IgG (1:800) (Molecular Probes), respectively. Slides were mounted with Vectashield mounting media with DAPI (Vector, H-1200) and sealed with nail makeup. Images were obtained with a Zeiss inverted fluorescent microscope coupled to an Axiocam hi-resolution digital camera operated by Axiovision 3.0 software (Carl Zeiss Inc., Thornwood, NY).

For detection of apoptosis in transiently transfected MCF-7 cells with hRad21 plasmids, the cells were first washed twice with ice-cold PBS and then fixed with cold methanol for 10 min. The fixed cells were washed again with PBS and mounted with Vectashield mounting media with DAPI (Vector, H-1200). At least 50 fluorescent nuclei from each treatment group were screened and counted for normal morphology (rounded chromatin) or for apoptotic nuclei (fragmented and condensed chromatin). Data were expressed as percentage of apoptotic cells out of total counted cells.

The caspase-3 activities in Molt4 cells were measured using a caspase-3 assay kit from Clontech (Palo Alto, CA) per manufacturer's protocol.

Proteolytic cleavage assay of the *in vitro* transcribed/translated hRad21: ^{35}S-hRad21 or unlabeled (non-isotopic) hRad21 was produced by *in vitro* transcription/translation using the TnT rabbit reticulocyte lysate system (Promega, WI, USA). Rabbit reticulocyte lysate was combined with 1μg of plasmid DNA containing either the WT *hRAD21* cDNA (pCS2MT-*hRAD21*) or *hRAD21* apoptotic cleavage site (ACS) mutants, ACS-mut-I or ACS-mut-II and SP6 RNA polymerase. Reaction in the absence of plasmid DNA served as a negative control. Reactions were incubated at 30^{0}C for 90 min. *In vitro* cleavage reaction was performed as previously described (9). In brief, 6 μl of *in vitro* translated ^{35}S-hRad21 (WT) or the ACS-mut-I or ACS-mut-II mutants were combined with 30 μl of reaction buffer (20 mM HEPES pH 7.4, 2 mM DTT, and 10% glycerol) and one of the following enzyme sources: 2 μl (200U) recombinant caspase-3, or 2 μl (4U) caspase-7 or 2 μl (10 μg) Molt4 cell lysates (treated with DMSO or 10 μM etoposide for 6h). The cleavage reaction was performed at 37^{0}C for 1h, after which 8 μl 6X sample buffer with DTT was added to stop the reaction. 20 μl of this reaction was electrophoresed on 6% SDS PAGE gels, fixed with methanol and acetic acid for 30 min, dried on a gel dryer and exposed to a STORM imager. Bands were quantified using the ImageQuant 5.2 software (Molecular Dynamics, Inc., Sunnyvale, CA). Unlabeled (non-isotopic) hRad21 from TnT reactions was also incubated in a similar manner as described above in the presence or absence of caspase-3 or caspase-7. Samples were then analyzed by SDS-PAGE followed by Western blotting with hRad21 antisera.

RESULTS

We report the role of hRad21 in the apoptotic response and cleavage of the hRad21 protein in human cells by a caspase-like activity.

Cleavage of hRad21 during apoptosis: While examining the expression of Rad21 in mammalian cells after DNA damage, we surprisingly identified cleavage of hRad21 protein after induction of apoptosis. hRad21 was cleaved during etoposide-induced apoptosis in human Molt4 T-cell leukemia. Induction of apoptosis resulted in the generation of approximately 64 kDa and 60 kDa cleavage products determined by a monoclonal hRad21 antibody (Fig. 1). The cleavage of hRad21 in Molt4 cells was a function of etoposide dose (Fig. 1A) as the ratio of cleaved hRad21 to full length protein appeared directly proportional to increasing doses of etoposide over the tested range (10-50 μM). hRad21 cleavage products were also detected in a number of other cell lines following induction of apoptosis either by DNA-damaging agents (ionizing radiation and topoisomerase inhibitors) (data not shown) and/or non-DNA-damaging agents (prostaglandin (Fig. 1B), proteasome inhibitor (Fig. 1C), cycloheximide treatment, and cytokine withdrawal, data not shown). In addition, equivalent doses of ionizing radiation in cells that are resistant to apoptosis (Raji lymphoid leukemia and H1299 large cell lung carcinoma) did not generate this band (data not shown); thus, it was not a simple by-product of DNA damage.

Translocation of the carboxy-terminal hRad21 fragment to the cytoplasm after induction of apoptosis: Molt4 cells were treated with 10 μM etoposide for 0, 1, 2, 3, 4, 6 and 12h. Induction of apoptosis was verified by determining caspase-3 activity (Fig. 2A) and the cleavage of PARP protein (data not shown). Western blot analysis of cytoplasmic and nuclear fractions using a C-

terminal hRad21 antibody detected a 122 kDa protein band in the non-induced cells (0 h), and as reported before, full length hRad21 is found to be exclusively in the nuclear fractions (Fig. 2B). However, induction of apoptosis resulted in the early (4h post induction) generation of approximately 64 kDa and 60 kDa cleavage products as determined by a C-terminal hRad21 antibody (Fig. 2B). At the end of 12h post induction, hRad21 protein is almost cleaved. Although hRad21 is a nuclear protein, the cleaved products are found in both nuclear and cytoplasmic fractions after induction of apoptosis (Fig. 2B). The identities of these two cleavage products were investigated using an N-terminal hRad21 antibody. As expected, the N-terminal antibody could not detect the 64 kDa and 60 kDa cleavage products either in the cytoplasmic or nuclear fractions. In contrast, this antibody detected two other bands (approximately 50 kDa and 55 kDa) only in the nuclear fractions (data not shown). These results indicated that hRad21 may potentially be cleaved at two different sites following induction of apoptosis. The C-terminal hRad21 cleavage products but not the N-terminal hRad21 products translocate to the cytoplasm after cleavage following induction of apoptosis.

The identities of the cleavage products were confirmed through recognition by monoclonal antibodies to hRad21 in immunoprecipitation (IP) and Western blot analyses (Fig. 3). Monoclonal hRad21 antibody selectively immunoprecipitated both the 60 kDa and 64 kDa hRad21 cleavage products, along with the native 122 kDa full length hRad21 protein in etoposide-induced Molt4 cells. Cells treated with vehicle only and control IP with isotype bacterial TrpE antibody did not detect hRad21 cleavage products, confirming the identities of the cleaved bands as hRad21 products. Both monoclonal and polyclonal C-terminal antibodies detected both the 64 kDa and 60 kDa bands, confirming these bands as the C-terminal portion of the cleaved protein.

Translocation of hRad21 was further investigated in EL-12 mammary epithelial cells by immunofluorescent staining using the monoclonal and the C-terminal hRad21 polyclonal antisera. Unlike Molt4 cells, EL-12 cells have a large cytoplasm to facilitate visualization. In these cells, Rad21 was entirely nuclear (Fig. 4, middle panel). Apoptosis was induced by treating EL-12 cells with UV light ($100J/m^2$) and was verified by the cleavage of Rad21 and PARP protein (data not shown). Immunofluorescent staining of the UV-treated cells by the C-terminal antibody clearly demonstrated translocation of the cleaved C-terminal Rad21 to the cytoplasm (Fig. 4, bottom panel).

Inhibition of hRad21cleavage by caspase peptide inhibitors: Peptide-based caspase inhibitors abrogated the apoptosis-induced cleavage of hRad21, suggesting the involvement of caspases in hRad21 cleavage (Fig. 5). Molt4 cells were treated with 20 μM z-VAD-FMK, a broad spectrum caspase inhibitor one hour prior to etoposide (10 μM) treatment. As shown in Fig. 5, treatment with z-VAD-FMK completely blocked etoposide-induced hRad21 cleavage. In an *in vitro* cleavage assay described later, z-VAD-FMK also inhibited caspase-3 induced cleavage of ^{35}S-hRad21 (data not shown).

Identification of the apoptotic cleavage site in hRad21: The hRad21 cleavage site was mapped through N-terminal sequencing of Coomassie-stained PVDF membranes that were electroblotted with immunoprecipitated hRad21 cleavage products (Fig. 6). Sequencing of the 64 kDa band revealed that hRad21 was cleaved at Asp (D)^{279}. The sequence obtained was SVDPVEP. The immediate sequence N-terminal to the cleavage site was PDSPD^{279}. Thus there was a repeat of the sequence encompassing the cleavage site, i.e., PDSPD^{279}/SVDPVEP (Fig.

6A). We were not successful in sequencing the 60 kDa band, possibly due to an N-terminal blocking effect. To verify whether specific cleavage occurred at Asp (D)^{279} in hRad21 after induction of apoptosis, we introduced a point mutation by substituting an alanine (A) for aspartate (D) at this position of hRad21(D279A) (Fig. 6B). Furthermore, because of the repetition of the cleavage sequence ^{275}PDSPDS^{280}, we made a second mutant by substituting alanine (A) for both aspartates (D) and serine (S) residues, i.e., hRad21 (^{275}PDSPDS^{280} to ^{275}PAAPAA^{280}). We then transiently transfected Molt4 cells with WT or mutant hRad21 tagged with the myc epitope at the N-terminus, and treated these cells with etoposide as indicated. As shown in Fig. 6C, antibody against myc-tag (9E10) revealed the proteins encoded by the transfected hRad21 WT and hRad21 ACS mut-I and ACS mut-II constructs. However, the cleavage fragments were only detected for WT hRad21, not for both of the mutants, indicating that a point mutation at Asp (D)^{279} prevented cleavage (Fig. 6C). We reprobed the blot with anti-hRad21 monoclonal Ab and found that both the 60 kDa and 64 kDa C-terminal fragments were present in all etoposide treated cells (data not shown), confirming that endogenous hRad21 was cleaved in cells transfected with hRad21 mutants.

Involvement of caspases in hRad21 cleavage: Closer inspection of the adjoining sequence at the Rad21 apoptotic cleavage site (D^{279}SVD) (Fig. 6A) revealed a putative recognition sequence for a primitive caspase Ced3. This sequence is conserved in vertebrates including human, mouse and frog (*Xenopus*). The sequence of the putative cleavage site, together with the inhibitory effect of a panel of caspase inhibitors on etoposide-induced apoptosis in Molt4 cells indicated the possible involvement of a caspase family protease. While the experiments with caspase inhibitors suggested involvement of a caspase family of protease(s) in the pathway leading to

hRad21 cleavage, they did not however demonstrate direct internal cleavage of hRad21 by a caspase. We therefore, utilized an *in vitro* cleavage assay as described previously for the retinoblastoma protein (Rb) (9) to examine the ability of purified caspase to cleave hRad21 (Fig. 7). We used two caspases, caspase-3 and caspase-7 that are major regulators of apoptosis in diverse cell types (35) (Fig. 7A), along with lysates from Molt4 cells treated with etoposide (apoptotic lysate) or vehicle (non-apoptotic lysate) to examine their role in hRad21 cleavage (Fig. 7B). Together, caspase-3 and caspase-7 comprise the caspase-3 subfamily and both enzymes recognize and cleave after the consensus cleavage site DXXD (1). Addition of recombinant caspase-3 or caspase-7 to the *in vito* transcribed and translated hRad21 in rabbit reticulocyte lysates clearly resulted in the production of a 64 kDa hRad21 fragment (Fig 7A, B). The 64 kDa fragment produced by these caspases precisely co-migrated with the 64 kDa band produce by apoptotic Molt4 lysates while the control (non-apoptotic) cell lysate could not cleave hRad21 protein. On the other hand, both the hRad21 ACS mutants failed to be cleaved by these two caspases or by apoptotic cell lysates in this assay, strongly suggesting that caspase-3 or caspase-7-like enzymes in the apoptotic cells or extracts were responsible for cleavage at the putative caspase recognition site D^{279} of hRad21.

In addition to the 64 kDa fragment, several other fragments were generated by caspase-3 and -7. It is possible that the 64 kDa fragment was degraded further by these caspases and resulted in the production of smaller fragments. In the presence of caspase-7 but not caspase-3, a 95 kDa fragment of hRad21 was also generated, suggesting another caspase site N-terminal to the D^{279} cleavage site. In the *in vitro* cleavage assay caspase-3 and -7 failed to generate the 60 kDa hRad21 fragment that accompanies the 64 kDa fragment after induction of apoptosis,

suggesting that the cleavage site generating the 60 kDa fragment was not recognized by caspase-3 and -7.

To determine whether caspase-3 is essential for the *in vivo* cleavage of hRad21, we utilized a caspase-3 deficient MCF-7 breast cancer cell line (21). In experiments using etoposide or tamoxifen-induced apoptosis in MCF-7 cells, hRad21 cleavage products were detected, indicating that caspase-3 was not essential for hRad21 cleavage (Fig. 8) and a caspase other than caspase-3 can act upon hRad21 to result in cleavage following induction of apoptosis.

hRad21 C-terminal cleavage product promotes apoptosis: A possible role for hRad21 in inducing apoptosis was first seen in preliminary experiments in which overexpression of hRad21 in Molt4 cells resulted in apoptotic phenotypes and enhanced expression of caspase-3 levels. As seen in Fig. 9, hRad21 overexpression from a CMV promoter–driven myc-tagged plasmid resulted in a 5-7 fold increase in caspase-3 activity compared to empty vector control. However, conclusive evidence for the role of cleaved hRad21 in promoting apoptosis was found in transiently transfected Molt4 cells with mammalian expression plasmids encoding the full length hRad21 or cDNAs encoding the two cleavage products, hRad21 N-terminal (aa 1-279) or hRad21 C-terminal (aa 280-631) proteins (Fig. 9). Although overexpression of WT hRad21 induced moderate levels of apoptosis as determined by caspase-3 activity in Molt4 cells, overexpression of hRad21 C-terminal cleavage product but not the N-terminal hRad21 cleavage product dramatically increased the caspase-3 activity in Molt4 cells (Fig. 9). The transfection efficiency in Molt4 was 35%, determined by a co-transfection with a red fluorescent plasmid pDSRed. Similar results were also obtained in hRad21 WT, hRad21 C-terminal and hRad21 N-terminal transfected MCF-7 cells. In these cells apoptosis was determined by monitoring the

phenotype of the DAPI stained nuclei. 40% of transfected cells had cellular and nuclear phenotypes typical of apoptosis, such as a round appearance with shrunken cell volume, chromatin condensation and nuclear disintegration (data not shown). These findings clearly demonstrated that the C-terminal hRad21 cleavage product was pro-apoptotic as determined by increased caspase-3 activity and apoptotic morphology and that its translocation to the cytoplasm may play a role in promoting apoptosis.

Apoptotic cleavage of hRad21 is not affected by the status of the p53 tumor suppressor protein in the cell: In view of the pivotal role of the p53 gene product in regulation of cell cycle and apoptosis, we examined the role of p53 in the apoptotic cleavage of hRad21. We used two myeloid leukemia cell lines ML-1 and HL-60 with WT and null p53 genotypes, respectively (32, 41). Apoptosis was induced using UV ($20J/m^2$) and ionizing radiation (20 Gy) in these cells. As shown in Fig. 10, in both the cell lines, induction of apoptosis resulted in the cleavage of hRad21 protein, indicating lack of a role for p53 in hRad21 cleavage.

DISCUSSION

Sister chromatid cohesion during DNA replication plays a pivotal role in accurate chromosomal segregation in the eukaryotic cell cycle. Rad21 is one of the major cohesin subunits that keeps sister chromatids together until anaphase when proteolytic cleavage by separase allows the chromosomes to separate. Mitotic cleavage sites in Rad21 in yeast as well as humans have been mapped (12, 37, 39). Here we show that hRad21 cleavage occurs during apoptosis and is induced by various agents including DNA damaging (ionizing radiation and topoisomerase inhibitors) as well as non-DNA damaging agents (cycloheximide treatment, cytokine withdrawal and treatment with proteasome inhibitors). We have biochemically mapped the apoptotic cleavage site in human Rad21 to PDSPD^{279}/S which is distinct from that of the mitotic cleavage sites (DREIMR^{172}/E and IEEPSR^{450}/L) previously described (12). The apoptotic cleavage site is conserved among vertebrate species, and it is likely that cleavage is mediated by a nuclear caspase or caspase-like molecule, as this cleavage site bears the characteristic caspase-3 subfamily recognition motif (DXXD) and hRad21 is cleaved *in vitro* by the two major apoptosis executioner caspases, caspase-3 and caspase-7. hRad21 cleavage is not restricted to transformed cancer cells, as induction of apoptosis also resulted in hRad21 cleavage in a primary cell line IMR90 (data not shown) as well as a non-transformed immortal cell line EL-12.

Cleavage of hRad21 appears to be an early event in the apoptotic pathway. The immunofluorescence experiments clearly demonstrate the translocation of the hRad21 C-terminal cleavage products to the cytoplasm early (3-4h post insult) in apoptosis. Early cleavage of

hRad21 and its translocation to the cytoplasm after induction of apoptosis and before the characteristic nuclear condensation and DNA fragmentation begin may have an important functional role in promoting and/or accelerating the apoptotic process. Indeed, our results clearly demonstrate that hRad21 proteolysis by a caspase family protease at D^{279}/S leads to the production of a pro-apoptotic C-terminal cleavage product. Translocation of this 64 kDa hRad21 cleavage product to the cytoplasm early in apoptosis may act as a nuclear signal that promotes and accelerates subsequent events of apoptosis. The specificity of this product was further determined as the N-terminal hRad21 cleavage product neither translocates nor has the ability to induce apoptosis. We have not explored the role of the 60 kDa hRad21 product generated at a cleavage site other than D^{279}/S, in the apoptotic process.

The physiological significance of cohesin hRad21 cleavage in apoptosis is intriguing. The nuclear signal (s) that detects subsequent events of apoptosis in the cytoplasm and mitochondria have remained elusive. It is possible that cleavage of hRad21 at the onset of apoptosis and the translocation of the C-terminal cleavage product to the cytoplasm acts as cues to accelerate the apoptotic process. We have previously identified a number of cytoplasmic proteins involved in the apoptotic pathway as interactors of the hRad21 protein in a yeast two-hybrid assay not described in the present study (Pati D, Plon SE, unpublished). These findings further strengthen the notion that the translocated C-terminal hRad21 protein plays a functional role in apoptosis.

Caspase-mediated proteolysis of hRad21 and the partial removal of hRad21 from the nucleus may expose the chromosomal DNA to DNAse and other proteins responsible for chromatin condensation and apoptotic DNA fragmentation. This simple scenario is less likely, as overexpression of the hRad21 ACS mutants, mut-I and mut-II did not prevent etoposide and tamoxifen-induced apoptosis and nuclear fragmentation in MCF-7 cells (data not shown). hRad21 was originally isolated in fission yeast as an essential protein with a role in DNA double strand break repair induced by ionizing radiation (3). It is therefore logical to think that disruption of the DNA repair function of hRad21 may be necessary during the execution of apoptosis. This notion has been strengthened with recent findings that a number of DNA repair enzymes such as Rad51 (15), ATM (13), DNA-PK (5), PARP (22) and cell cycle regulators such as Rb (9) are cleaved by caspases. Coordinated destruction of the DNA repair machinery and cell cycle regulators by the caspase family of proteases therefore constitutes a physiologically relevant process that promotes and accelerates chromosomal condensation and DNA fragmentation without interference by the cell cycle and DNA repair machinery. Unlike hRad21, however, cleavage products of these other DNA repair proteins have not been reported to play a direct role in promoting apoptosis. In this case, cleavage of hRad21 by caspases may play a unique role in amplifying the apoptotic signal by elevating the level of caspase activity (Fig. 11). A similar mechanism for amplifying the apoptotic signal for caspase substrate vimentin has recently been described (4).

The p53 tumor suppressor protein plays a central role in the regulation of the cell cycle and apoptosis after DNA damage (17, 34). In the event that DNA damage is more severe and non-repairable, p53 directs the cells into apoptosis through the Bax/Bcl-2 pathway. p53 status

does not appear to have any effect on the apoptotic cleavage of hRad21 after DNA damage (i.e. UV and IR), indicating the lack of involvement of the p53 pathway in hRad21 cleavage. It is possible that a parallel p53-independent pathway may regulate the genotoxic-damage induced hRad21 cleavage.

Finally, it is interesting to note that cleavage of cohesin hRad21 is carried out by a separase in mitosis and by a caspase in apoptosis at different sites in the protein. Both these proteases belong to the distantly related CD-clan protease family (38), suggesting an evolutionarily conserved mechanism shared by the mitotic and apoptotic machinery. hRad21 may serve as the link between the two key cellular processes of mitosis and apoptosis. In summary, in contrast to previously described functions of Rad21, in chromosome segregation and DNA repair, cleavage of the cohesion protein and translocation of the C-terminal cleavage product to the cytoplasm are early events in the apoptotic pathway that amplify the apoptotic signal in a positive feed back manner by activating more caspases. These results provide the framework to identify the physiologic role of hRad21 in the apoptotic response in normal and malignant cells.

ACKNOWLEDGEMENTS

We thank T. Nagase (Kazusa DNA Research Institute, Chiba, Japan) for KIAA0078 (SK-hRad21) plasmid, J-M. Peters (Research Institute of Molecular Pathology, Vienna, Austria) for Rad21 N-terminal polyclonal antibody and D. Medina (Baylor College of Medicine) for EL-12 cell line. We thank Lisa Wang for critically reading the manuscript and Sara Ekhlassi for technical assistance.

This study was supported by grants from the U.S. Army Medical Research and Materiel Command (DAMD-17-00-1-0606, DAMD-01-1-0142 and DAMD 01-1-0143 to DP) and (DAMD-17-97-1-7284 and DAMD-17-98-1-8281 to SEP.

REFERENCES

1. Alnemri, E., S. D. J. Livingston, D. W. Nicholson, G. Salvesen, N. A. Thornberry, W. W. Wong, and J. Yuan. 1996. Human ICE/CED-3 protease nomenclature. Cell **87:**171.

2. Biggins, S., and A. W. Murray. 1999. Sister chromatid cohesion in mitosis. Curr. Opin. Genet. Dev. **9:**230-236.

3. Birkenbihl, R. P., and S. Subramani. 1992. Cloning and characterization of rad21 an essential gene of *Schizosaccharomyces pombe* involved in DNA double-strand-break repair. Nucleic Acids Res. **20:**6605-6611.

4. Byun, Y., F. Chen, R. Chang, M. Trivedi, K. J. Green, and V. L. Cryns. 2001. Caspase cleavage of vimentin disrupts intermediate filaments and promotes apoptosis. Cell Death Differ. **8:** 443-450.

5. Casciola-Rosen, L. A., G. J. Anhalt, and A. Rosen. 1995. DNA-dependent protein kinase is one of a subset of autoantigens specifically cleaved early during apoptosis. J. Exp. Med. **182:**1625-1634.

6. Chaturvedi, M. M., R. LaPushin, and B. B. Aggarwal. 1994. Tumor necrosis factor and lymphotoxin. Qualitative and quantitative differences in the mediation of early and late cellular response. J. Biol. Chem. **269:**14575-14583.

7. Ciosk, R., W. Zachariae, C. Michaelis, A. Shevchenko, M. Mann, and K. Nasmyth. 1998. An ESP1/PDS1 complex regulates loss of sister chromatid cohesion at the metaphase to anaphase transition in yeast. Cell **93:**1067-1076.

8. Cohen-Fix, O., J-M. Peters, M. W. Kirschner, and D. Koshland. 1996. Anaphase initiation in Saccharomyces cerevisiae is controlled by the APC-dependent degradation of the anaphase inhibitor Pds1p. Genes Dev. **10:**3081-93.

9. Fattman, C. L., S. M. Delach, Q. P. Dou, and D. E. Johnson. 2001. Sequential two-step cleavage of retinoblastoma protein by caspase-3/-7 during etoposide-induced apoptosis. Oncogene **20:**2918-2926.

10. Funabiki, H., H. Yamano, K. Kumada, K. Nagao, T. Hunt, and M. Yanagida. 1996. Cut2 proteolysis required for sister-chromatid seperation in fission yeast. Nature **381:**438-441.

11. Guacci, V., D. Koshland, and A. Strunnikov. 1997. A direct link between sister chromatid cohesion and chromosome condensation revealed through the analysis of MCD1 in *S. cerevisiae*. Cell **9:**47-57

12. Hauf, S., I. C. Waizenegger, and J-M. Peters. 2001. Cohesin cleavage by separase required for anaphase and cytokinesis in human cells. Science **293:**1320-1323.

13. Hotti, A., K. Jarvinen, P. Siivola, and E. Holtta. 2000. Caspases and mitochondria in c-Myc-induced apoptosis: identification of ATM as a new target of caspases. Oncogene **19:**2354-2362.

14. Huang, D. C. S., L. A. O'Reilly, A. Strasser, and S. Cory. 1997. The anti-apoptosis function of bcl-2 can be genetically separated from its inhibitory effect on cell cycle entry. EMBO J. **16:**4628-4638.

15. Huang, Y., S. Nakada, T. Ishiko, T. Utsugisawa, R. Datta, S. Kharbanda, K. Yoshida, R. V. Talanian, R. Weichselbaum, D. Kufe, and Z. M. Yuan. 1999. Role for caspase-mediated cleavage of Rad51 in induction of apoptosis by DNA damage. Mol. Cell Biol. **19:**2986-2997.

16. Hunter, T. 1997. Oncoprotein network. Cell **88**:333-346.

17. Isreals, L. G., and E. D. Isreals. 1999. Apoptosis. Stem Cells **17**:306-313.

18. Jallepalli, P. V., I. C. Waizenegger, F. Bunz, S. Langer, M. R. Speicher, J-M. Peters, K. W. Kinzler, B. Vogelstein, and C. Lengauer. 2001. Securin is required for chromosomal stability in human cells. Cell **105:**445-457

19. Keelan, J. A., T. A. Sato, K. W. Marvin, J. Lander, R. S. Gilmour, and M. D. Mitchell. 1999. 15-deoxy-delta 12, 14-prostaglandin J_2, a ligand for peroxisome proliferator-activated receptor-g, induces apoptosis in JEG3 choriocarcinoma cells. Biochem. Biophys. Res. Comm. **262:**579-585.

20. Koshland, D. E., and V. Guacci. 2000. Sister chromatid cohesion: the beginning of a long and beautiful relationship. Curr. Opin. Cell Biol. **12:**297-301.

21. Kurokawa, H., K. Nishio, H. Fukumoto, A. Tomonari, T. Suzuki, and N. Saijo. 1999. Alteration of caspase-3 (CPP32/Yama/apopain) in wild-type MCF-7, breast cancer cells. Oncol. Rep. **6:**33-37.

22. Lazebnik, Y. A., S. H. Kaufmann, S. Desnoyers, G. G. Poirier, and W. C. Earnshaw. 1994. Cleavage of poly (ADP-ribose) polymerase by a proteinase with properties like ICE. Nature **371:**346-347.

23. Leismann, O., A. Herzig, S. Heidmann, and C. F. Lehner. 2000. Degradation of Drosophila PIM regulates sister chromatid separation during mitosis. Genes. Dev. 2000 **14:**2192-205.

24. Levine, A. J. 1997. p53, the cellular gatekeeper for growth and division. Cell **88:**323-331.

25. Lipponen, P., S. Aaltomaa, V-M. Kosma, and K. Syrjanen. 1994. Apoptosis in breast cancer as related to histopathological characteristics and prognosis. Eur. J. Cancer **30A:**2068-2073.

26. Losada, A., and T. Hirano. 2001. Shaping the metaphase chromosome: coordination of cohesion and condensation. Bioessays **23:**924-935.

27. Medina, D., and F. S. Kittrell. 1993. Immortalization phenotype dissociated from the preneoplastic phenotype in mouse mammary epithelial outgrowths *in vivo*. Carcinogenesis **14:**25-28.

28. Michaelis, C., R. Ciosk, and K. Nasmyth. 1997. Cohesins: Chromosomal proteins that prevent premature seperation of sister chromatids. Cell **91:**35-45.

29. Minn, A. J., L. H. Boise, and C. B. Thompson. 1996. Expression of Bcl-X_l and loss of p53 can cooperate to overcome a cell cycle checkpoint induced by mitotic spindle damage. Genes Dev. **10:**2621-2631.

30. Nasmyth, K., J-M. Peters, and F. Uhlmann. 2000. Splitting the chromosome: cutting the ties that bind sister chromatids. Science **288**:1379-1385.

31. Nasmyth, K. 2001. Disseminating the genome: joining, resolving, and separating sister chromatids during mitosis and meiosis. Annu. Rev. Genet. **35:**673-745.

32. O'Connor, P. M., J. Jackman, I. Bae, T. G. Myers, S. Fan, M. Mutoh, D. A. Scudiero, A. Monks, E. A. Sausville, J. N. Weinstein, S. Friend, A. J. Fornace Jr., and K. W. Kohn. 1997. Characterization of the p53 tumor suppressor pathway in cell lines of the National Cancer Institute anticancer drug screen and correlations with the growth-inhibitory potency of 123 anticancer agents. Cancer Res. **57:**4285-300.

33. Shimada, A. 1996. PCR-based site-directed mutagenesis. Methods Mol. Biol. **57:**157-165.

34. Strasser, A., L. O'Connor, and V. M. Dixit. 2000. Apoptosis Signaling. 2000. Annu. Rev. Biochem. **69:**217-245.

35. Thornberry, N. A., Y. Lazebnik. 1998. Caspases: enemies within. Science **281:**1312-1316.

36. Uhlmann, F., and K. Nasmyth. 1998. Cohesion between sister chromatids must be established during DNA replication. Curr. Biol. **8:**1095-1101.

37. Uhlmann, F., F. Lottspeich, and K. Nasmyth. 1999. Sister chromatid separation at anaphase onset is promoted by cleavage of the cohesin subunit Scc1. Nature **400:** 37-42.

38. Uhlmann, F., D. Wernic, M. A. Poupart , E. V. Koonin, and K. Nasmyth. 2000. Cleavage of cohesin by the CD clan protease separin triggers anaphase in yeast. Cell **103:** 375-386.

39. Waizenegger, I. C., S. Hauf, A. Meinke, and J-M. Peters. 2000. Two distinct pathways remove mammalian cohesin from chromosome arms in prophase and from centromeres in anaphase. Cell **103:**399-410.

40. Warren, W. D., S. Steffensen, E. Lin, P. Coelho, M. Loupart, N. Cobbe, J. Y. Lee, M. J. McKay, T. Orr-Weaver, M. M. Heck, and C. E. Sunkel. 2000. The Drosophila RAD21 cohesin persists at the centromere region in mitosis. Curr. Biol. **10:**1463-1466.

41. Zhan, Q., S. Fan, I. Bae, C. Guillouf, D. A. Liebermann , P. M. O'Connor, and A. J. Fornace. 1994. Induction of bax by genotoxic stress in human cells correlates with normal p53 status and apoptosis. Oncogene **9:**3743-51.

42. Zou, H, T. J. McGarry, T. Bernal, and M. W. Kirschner. 1999. Identification of a vertebrate sister-chromatid separation inhibitor involved in transformation and tumorigenesis. Science **285:**418-22.

FIGURE LEGENDS

Fig. 1. Apoptosis-induced cleavage of hRad21 by etoposide (A), prostaglandin (B) and proteasome inhibitors (C) in Molt4 T-cell leukemia and JEG3 choriocarcinoma cells. (A). Dose-related cleavage of hRad21 in Molt4 T-cell leukemia, treated with increasing concentration of etoposide (10-50 μM) for 6h and (B) JEG3 cells with 15-deoxy-delta 12, 14-prostaglandin J_2 (2.4-8 μM) for 16h. (C) Molt 4 cells were also treated with 0.025 mM proteasome inhibitors, MG115 and MG132 for 8h. Lysates of these samples were resolved on a 4-20% SDS-PAGE gel, transferred to a nitrocellulose membrane and analyzed by Western blot using a monoclonal hRad21 antibody. Induction of apoptosis resulted in the generation of approximately 64 kDa and 60 kDa hRad21 cleavage products (shown by the closed arrows). Full length hRad21 (122 kDa) is shown by the open arrow.

Fig. 2. Time course of etoposide-induced hRad21 cleavage. Molt4 cells were incubated in the absence (lane 1) or presence of 10μM etoposide for 1, 2, 3, 4,6 and 12 hours. At the end of the incubation period lysates from cytoplasmic and nuclear fractions were made. (A) Induction of apoptosis was verified by determining caspase-3 activity in a Western blot analysis using anti-caspase-3 monoclonal antibody. Pro-caspase-3 and the active caspase-3 are indicated. (B) Time course of cleavage of hRad21 protein in etoposide-induced cytoplasmic and nuclear fractions were examined using a C-terminal Rad21 pAb. Full

length hRad21 (122 kDa, open arrow), C-terminal cleaved 60 and 64 kDa fragments (closed arrows) are indicated.

Fig. 3. Immunoprecipitation (IP) and Western blot (WB) analyses of the hRad21 cleavage products. Apoptosis was induced in Molt4 T-cells by treating with 10 μM etoposide (etop) for 8h. Protein lysates were subjected to immunoprecipitation using hRad21 mAb or a control bacterial trpE mAb. Both monoclonal and polyclonal C-terminal antibodies detected both 64 kDa and 60 kDa bands (closed arrows), indicating these bands are from the C-terminal portion of the cleaved protein.

Fig. 4. C-terminal Rad21 cleavage product translocates to the cytoplasm after induction of apoptosis. Apoptosis was induced by treating EL-12 mammary epithelial cells with UV light ($100J/m^2$). UV-treated (bottom panel) and untreated control (middle panel) cells were subjected to immunofluorescent staining and microscopy using a C-terminal hRad21 polyclonal antibody (pAb) (green fluorescence) and hRad21 monoclonal antibody (mAb) (red fluorescence), respectively. The signals of mAb and pAb were visualized by adding rhodamine-labeled goat anti-mouse and fluorescein-labeled goat anti-rabbit IgG, respectively. Upper panel is the background staining (negative control) from the fluorescein-labeled secondary antibody in the present of normal mouse and rabbit IgG. The nuclear material is visualized by DAPI staining (blue fluorescence). Right hand panel is a merged image of red, blue and green fluorescence.

Fig. 5. Caspase peptide inhibitors inhibit etoposide-induced cleavage of hRad21. Molt4 cells were treated with 20 μM z-VAD-FMK, a broad spectrum caspase inhibitor one hour prior to etoposide (10 μM) treatment for 6 hours. At the end of the incubation period protein lysates were analyzed on a 6% SDS-PAGE gel followed by Western blot analysis using hRad21 C-terminal pAb.

Fig. 6. Characterization of the apoptotic cleavage site of hRad21. hRad21 cleavage site was mapped biochemically as described in the Methods section through N-terminal sequencing of Coomassie-stained PVDF membrane that was electroblotted with immunoprecipitated hRad21 cleavage products. (A) Comparison of the apoptotic cleavage recognition site and the adjoining sequence of hRad21 with other vertebrates (Mouse and *Xenopus*) and simpler eukaryotic Rad21 proteins. An arrow indicates the peptide bond cleaved during apoptosis. (B) Construction of the apoptotic cleavage site mutants, ACS mut-I and ACS mut-II, to verify whether specific cleavage occurs at Asp $(D)^{279}$ in hRad21 after induction of apoptosis, by introducing a point mutation to substitute an alanine (A) for aspartate (D) (mut-I) or alanine (A) for aspartate (D) and serine (S) (mut-II). (C) Molt4 cells were transiently transfected with blank vector (pCS2MT), WT hRad21 (pCS2MT-*hRAD21*) or ACS mutants tagged with myc epitope at their N-termini (pCS2MT-ACSmut-I or pCS2MT-ACSmut-II), and treated these cells with etoposide as indicated. Lysates were analyzed on 6% SDS-PAGE followed by Western blot analysis using antibody against myc-tag (9E10) to distinguish the cleavage products from the native forms of transfected hRad21 WT and hRad21 ACS mut-I and ACS mut-II proteins.

Fig. 7. Cleavage of *in vitro* translated hRad21 by recombinant caspase-3 and caspase-7. (A) In a cleavage reaction, *in vitro* translated unlabeled (non-isotopic) hRad21WT or hRad21 apoptotic cleavage site (ACS) mutants, ACSmut-I or ACSMut-II in the rabbit reticulocyte lysate were incubated with saline (vehicle) (lane a) or with caspase-3 (lane b) or caspase-7 (lane c). TnT reactions in the absence of plasmid DNA served as a negative control. Samples were analyzed on a 6% SDS PAGE followed by Western blotting with hRad21 C-terminal pAb. (B) ^{35}S-hRad21 was incubated in the absence of extract (lane 1) and presence of Molt4 cell lysates treated with DMSO (lane 2) or 10μM etoposide for 6h (lane 3). Samples were resolved on a 6% SDS-PAGE gel, fixed with methanol and acetic acid for 30 min, dried on a gel dryer and exposed to a STORM imager.

Fig. 8. Cleavage hRad21 in the Caspase-3 deficient MCF-7 breast cancer cells. Apoptosis was induced by treating MCF-7 cells with 60 μM etoposide for 6h. Cells treated with DMSO (vehicle) served as a control. Whole cell lysates or lysates from the cytoplasmic and nuclear fractions were electrophoresed on a 6% SDS-PAGE gel and subjected to Western blot analysis using hRad21 mAb. Arrows indicate the hRad21 products.

Fig. 9. C-terminal hRad21 cleavage product promotes apoptosis in Molt4 T-cell leukemia. Molt4 cells were transiently transfected with CMV promoter–driven myc-tagged mammalian expression plasmids encoding the full length hRad21 or cDNAs encoding the two cleavage products, hRad21 N-terminal (aa 1-279) or hRad21 C-terminal (aa 280-631)

proteins. Caspase-3 activity was measured as described in the methods section. Data are the averages and standard error of the means from two experiments.

Fig. 10. Effect of p53 status on the cleavage of hRad21. Apoptosis was induced in myeloid leukemia cell lines ML-1 and HL-60 with WT and null p53 genotypes, respectively, by treating the cells with ultraviolet (UV) light (20 J/m^2) or ionizing radiation (IR) (20 Gy). Six hour after treatment, protein lysates were made and resolved on a 6% SDS-PAGE followed by Western blot analysis using hRad21 monoclonal antibody. Arrows indicate hRad21 cleavage products. C= control without the UV or IR treatment.

Fig. 11. Model showing the cleavage of the cohesion protein hRad21 and translocation of the C-terminal cleavage product to the cytoplasm early in the apoptotic pathway that amplifies the cell death signal in a positive feed back manner by activating more caspases.

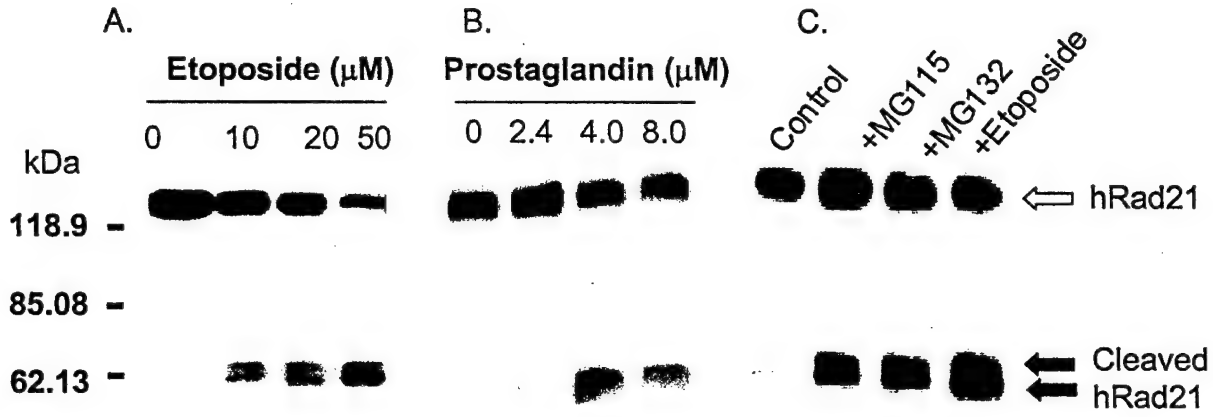
A.
Etoposide (μM)
0 10 20 50
B.
Prostaglandin (μM)
0 2.4 4.0 8.0
C.
Control
+MG115
+MG132
+Etoposide
kDa
118.9
85.08
62.13
hRad21
Cleaved
hRad21

Fig. 1

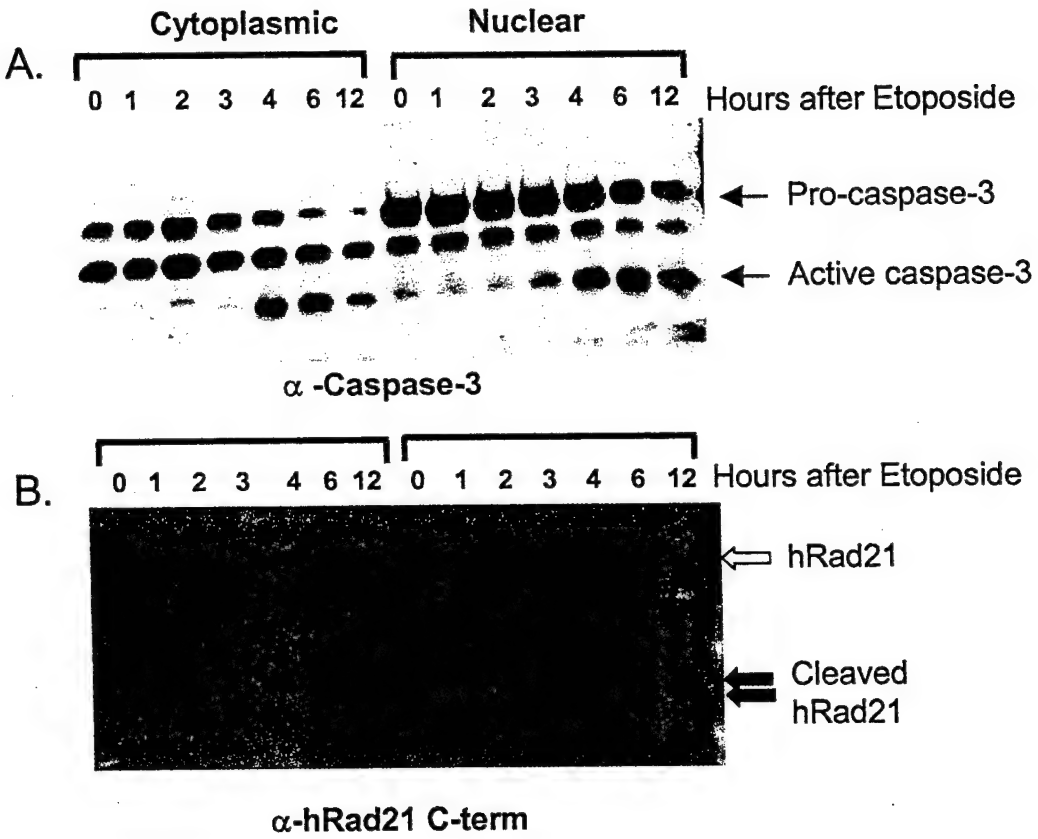
A.
Cytoplasmic
Nuclear
0 1 2 3 4 6 12 0 1 2 3 4 6 12
Hours after Etoposide
Pro-caspase-3
Active caspase-3
α -Caspase-3
B.
0 1 2 3 4 6 12 0 1 2 3 4 6 12
Hours after Etoposide
hRad21
Cleaved
hRad21
α-hRad21 C-term

Fig. 2

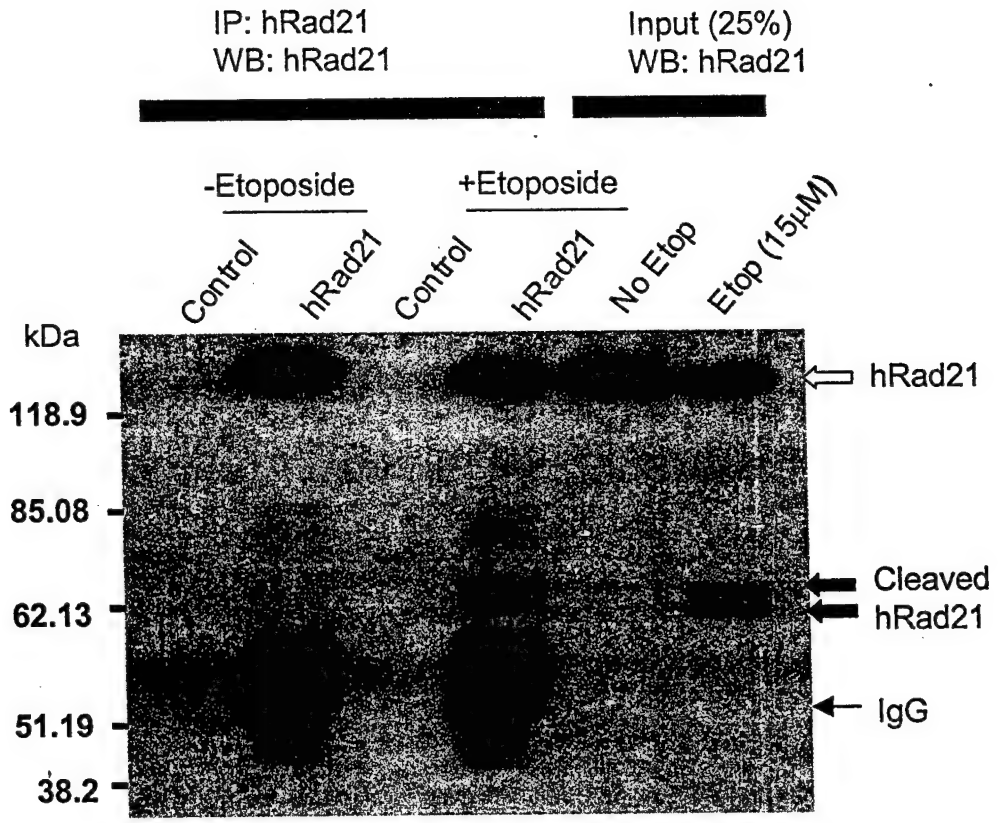
IP: hRad21
WB: hRad21
Input (25%)
WB: hRad21
-Etoposide
+Etoposide
Control
hRad21
Control
hRad21
No Etop
Etop (15μM)
kDa
118.9
85.08
62.13
51.19
38.2
hRad21
Cleaved
hRad21
IgG

Fig. 3

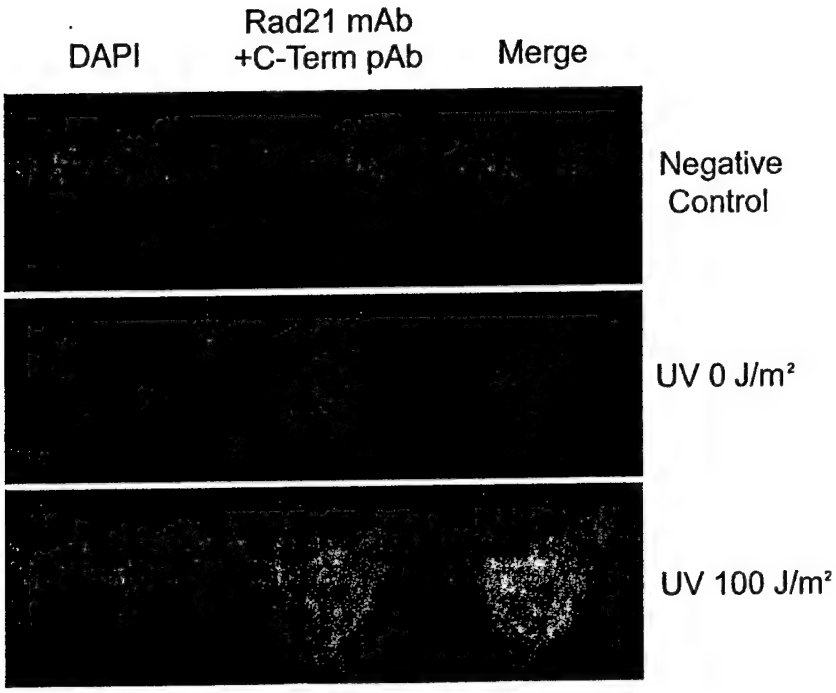
DAPI
Rad21 mAb
+C-Term pAb
Merge
Negative
Control
UV 0 J/m²
UV 100 J/m²

Fig. 4

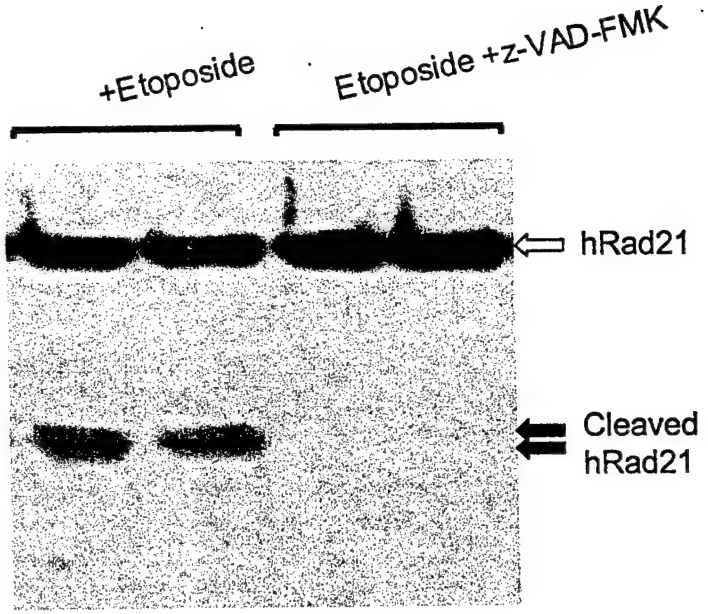

Fig. 5

A.

```
HumanRad21            267 ------------DDNVSMGGPDSPDSVDPVEPMPTMTDQTTLVPNEEEAFALEPIDITVKE---TKAKRKRKLIVDSVKE
MouseRad21            267 ------------DDNGSLGGPDSPDSVDPVEPMPTMTDQTTLVPNEEEAFALEPIDITVKE---TKAKRKRKLIVDSVKE
Xenopus Rad21         265 ------------DDNVSMGAPDSPDSVDPVEPLPTMTDQTTLVPNEEEAFALEPIDITVKE---TKAKRKRKLIVDSVKE
Arabidopsis Rad21     259  TLNEKEPTI SIDEEMLNS RHSAFELRS SPGSAAGSE ERADFVHPS QLVLQPSPP Q---PQRRA KRKNFDGVT
Drosophila Rad21      268 VPSPATSLVNSIEDEKEENNLNGHASVSENVPMN----EITLVQNEDEGFALAPLDVSMYKGV-TKAKRKRKLIIDEIKN
C.elegans Rad21       269 HP----------VREHAVADVQNDDGMDFDYQPFEPENVEPSRPQSPESFALEPLDVEHMEGRKKRQRKARKLIVDAETM
Fission Yeast Rad21   251 L DLG------ -LDDLLGDQ GANAPAIE  EQAETSSIL PSDIMEDDS RPAAAGVEG QVVESATAQ QEKINPQK
Budding Yeast Rad21   216 W DLG------ ----ITEKD QNNDDDDN  EQGRRLGEI MSEEPTDFF DLDIEKEAA G-------N IDTITDAM
consensus             321              d   mg       vd              v ne e falepiditv      k kr rklivd
```

B.

Wild Type

ATG GGT GGG CCT GAT AGT CCT GAT TCA GTG GAT
M G G **P** **D** **S** P **D** **S** V D

279

ACS Mutant-I

ATG GGT GGG CCT GAT AGT CCT **GCT** TCA GTG GAT
M G G P D S P **A** S V D

ACS Mutant-II

ATG GGT GGG CCT **GCT** **GCT** CCT **GCT** **GCA** GTG GAT
M G G P **A** **A** P **A** **A** V D

C.

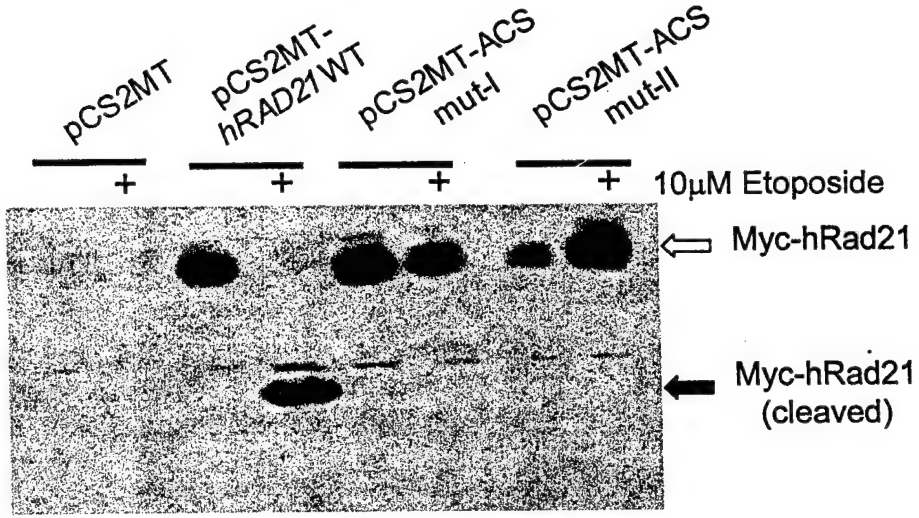

Fig.6

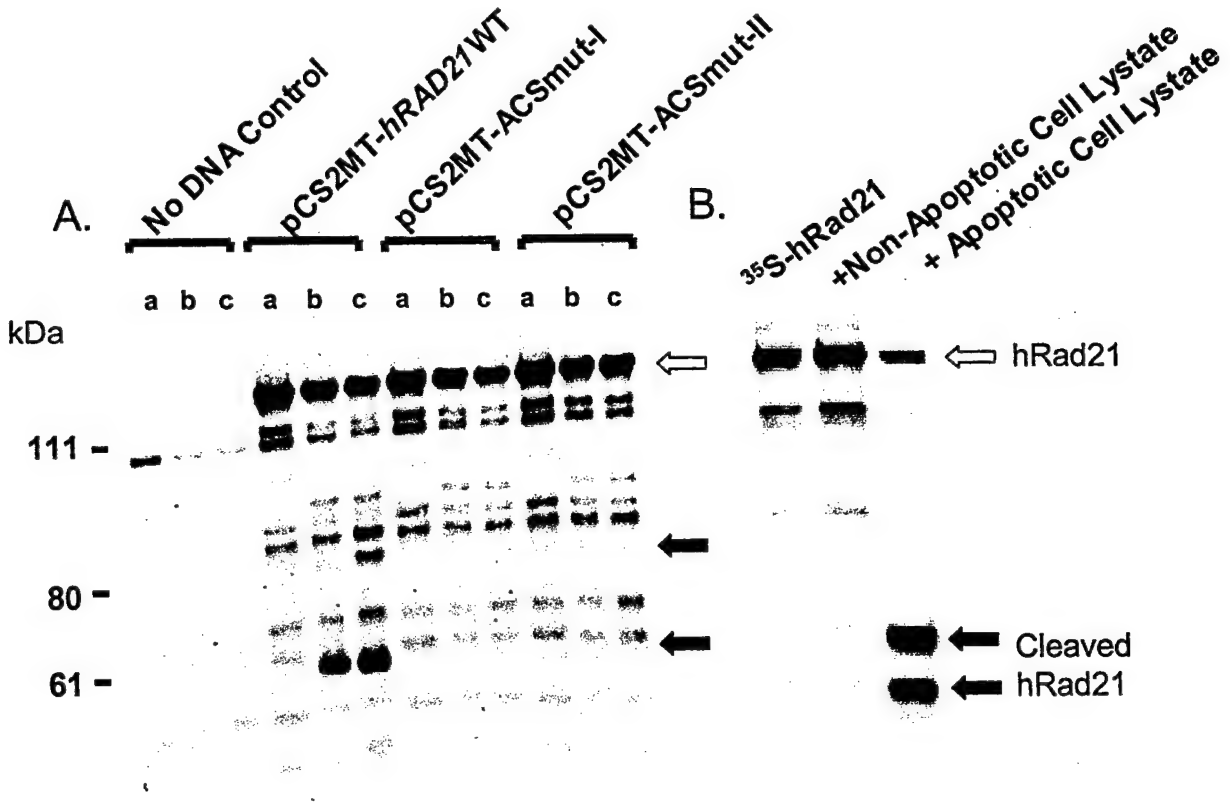

a = +vehicle, b = +caspase-3, c = +caspase-7

Fig. 7

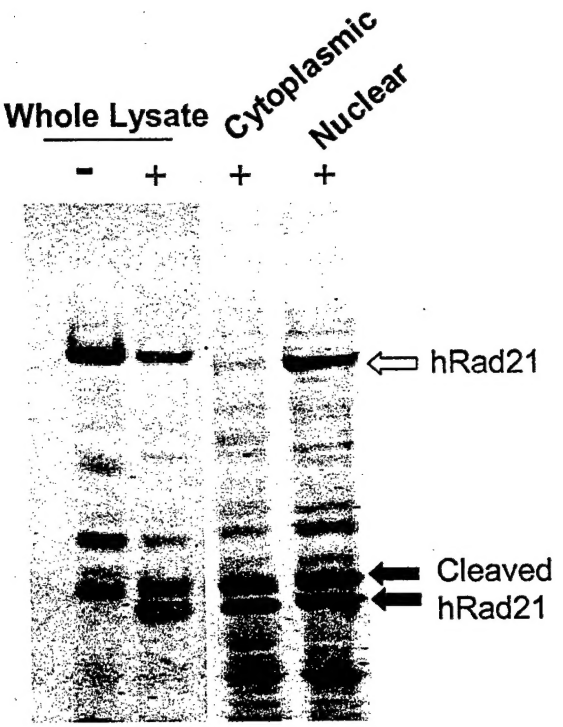
Whole Lysate
Cytoplasmic
Nuclear
-
+
+
+
hRad21
Cleaved
hRad21
+ 60 μm Etoposide (6h)

Fig. 8

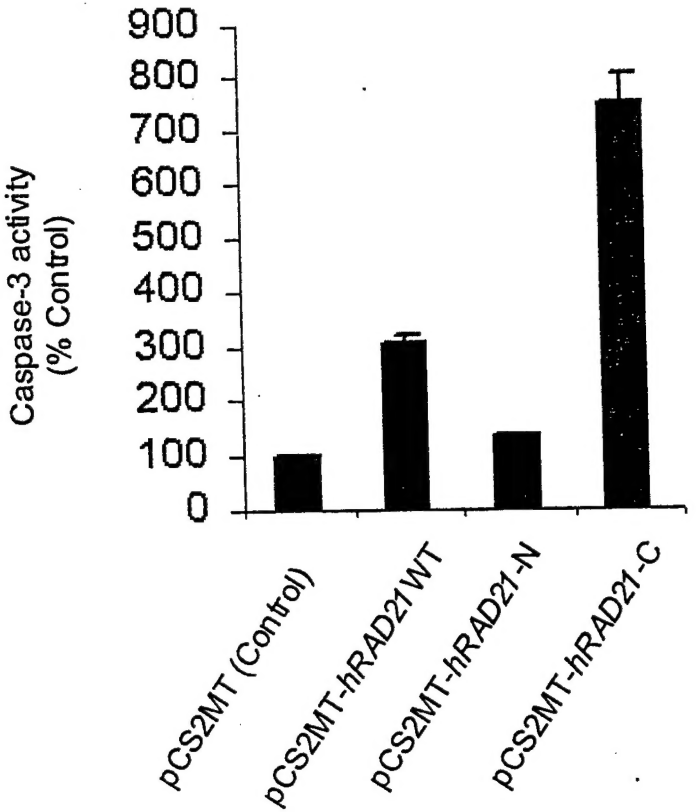
Caspase-3 activity
(% Control)
900
800
700
600
500
400
300
200
100
0
pCS2MT (Control)
pCS2MT-hRAD21WT
pCS2MT-hRAD21-N
pCS2MT-hRAD21-C

Fig. 9

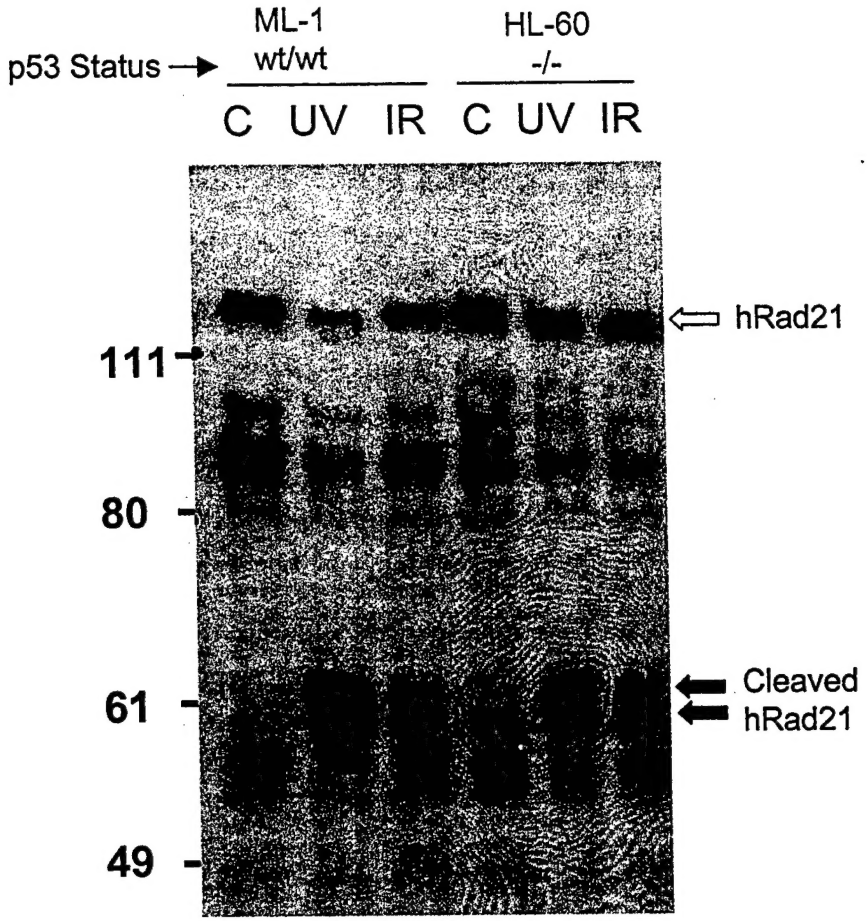
p53 Status
ML-1
wt/wt
HL-60
-/-
C UV IR C UV IR
111
80
61
49
hRad21
Cleaved
hRad21

Fig. 10

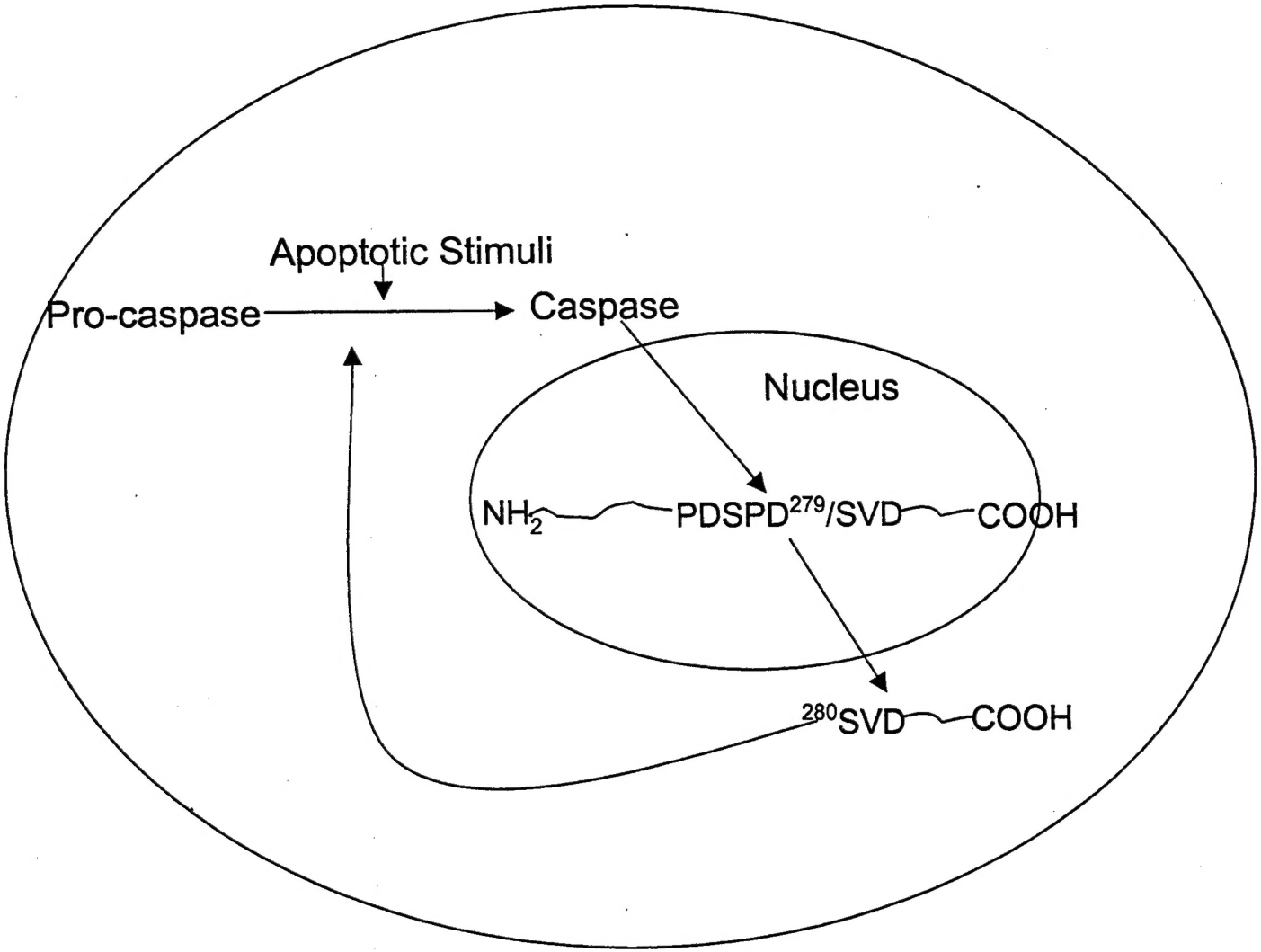
Apoptotic Stimuli
Pro-caspase
Caspase
Nucleus
NH2
PDSPD279/SVD
COOH
280SVD
COOH

Fig. 11